

**Flood Control**  
**2015**

**SOLUTIONS FOR SMART FLOOD CONTROL**



**EXTRAPOLATION ERROR OF  
PEAK WATER LEVELS FROM  
UNCERTAIN FLOODPLAIN  
ROUGHNESS IN 2D  
HYDRODYNAMIC MODELS**

## INFO

### Title

Extrapolation error of peak water levels from uncertain floodplain roughness in 2D hydrodynamic models

### Commissioned by

Stichting Flood Control

### Number of pages

66

### Status

Final

Version	Date	Author	Signature	Reviewer	Signature
2	2012-01-23	M.W. Straatsma F. Huthoff			

### Research team:

- > UT-ITC dr. M.W. Straatsma
- > HKV, dr. F.Huthoff

### Disclaimer

While every effort has been made to ensure that the information herein is accurate, Stichting Flood Control does not accept liability for error or fact or opinion which may be present, nor for the consequences of any financial decision based on this information. The reports and material submitted by the various research providers, which are contained within the publication, have been prepared in accordance with reasonable standards of scientific endeavor. The research providers also have no control over its use by third parties, and shall likewise have no liability to a third party arising from their use of this information.

## MANAGEMENT SUMMARY

Uncertainty in water levels at the design discharge has a large number of causal factors. In this report, we address the error due to uncertainty in floodplain roughness parameterization. We looked at different aspects. Firstly, we used the current ecotope map and the error matrix from the field validation to determine the uncertainty. We created 15 ecotope maps at two different classification accuracies and ran a 2D hydrodynamic model to assess the uncertainty in water levels and discharge distribution at nine different stationary discharges. We found a linear increase in the spread in the model outcome with increasing discharge. The spread ranged from less than a cm at 3500 m<sup>3</sup>/s to 19 cm at 16,000 m<sup>3</sup>/s. The discharge varied up to 95 m<sup>3</sup>/s over the two bifurcation points in the Rhine branches in The Netherlands. In the second part, we looked at the extrapolation error beyond the historic flood event of 12,000 m<sup>3</sup>/s in 1995. We looked at the additional variation in flood water levels between the calibration discharge and the design discharge of 16,000 m<sup>3</sup>/s. The additional variation is approximately 50% of the spread that we found when calibration was not taken into account. The preliminary results of a newly developed analytic method to correct the variation indicated that the extrapolation error due to floodplain vegetation roughness resulting from classification errors is less than 4 cm.

Lastly, the uncertainty in operational flood forecasting was assessed. The benchmark for the predicting accuracy is 10, 15, 25 and 40 cm for the 1-4 day lead time, respectively. This shows that the desired accuracy of 10, 15, 20, and 40 cm prediction accuracy for the 1-4 day forecast is not always reached. One day forecasts are within the desired accuracy 81 % of the time, while the 3 and 4 day forecasts proved to be accurate only 49, and 54 % of the time, respectively.

# TABLE OF CONTENTS

<b>Management summary .....</b>	<b>3</b>
<b>Table of contents.....</b>	<b>4</b>
<b>1 Introduction.....</b>	<b>5</b>
<b>2 Floodplain roughness .....</b>	<b>8</b>
2.1 Uncertainty in floodplain roughness .....	8
2.2 Roughness parameterization in WAQUA .....	9
2.3 Classification error in ecotope maps.....	10
<b>3 Study area .....</b>	<b>13</b>
<b>4 Methods.....</b>	<b>15</b>
4.1 New realizations of ecotope maps.....	15
4.2 Hydrodynamic modeling .....	18
4.3 Prediction uncertainty in operational flood forecasting .....	19
<b>5 Results.....</b>	<b>20</b>
5.1 Uncertainty in hydrodynamics relative to flow rate .....	20
5.2 Extrapolation error .....	24
5.3 Current prediction accuracy.....	32
<b>6 Discussion.....</b>	<b>36</b>
<b>7 Conclusions and recommendations.....</b>	<b>39</b>
References.....	40
<b>Appendix 1 : Adjusted error matrix .....</b>	<b>43</b>
<b>Appendix 2 : ecotopes Baseline 4 roughness codes.....</b>	<b>48</b>
<b>Appendix 3 : Overview of figures.....</b>	<b>51</b>
<b>Appendix 4 : Extrapolation error in water levels.....</b>	<b>55</b>
<b>Appendix 5 : Extrapolation error in discharge .....</b>	<b>58</b>
<b>Appendix 6 : Uncertainty bounds of extrapolated water levels .....</b>	<b>62</b>
6.1 Procedure P1 (with calibration) .....	62
6.2 Procedure P2 (without calibration).....	63
6.3 Quantification of the proportionality factor f for the Rhine branches.....	65
6.4 Conclusion.....	65

# 1 INTRODUCTION

Water level predictions of large rivers provide important information for shipping and operational water management. Enhanced ability to forecast peak discharges remains the most relevant nonstructural measure for flood protection (Reggiani and Weerts, 2008). It enables to take mitigating measures like sand bagging of embankments, or initiation of evacuation plans. A high accuracy is desired in flood peak prediction as mitigating measures can be costly and disruptive to society. As complete determinism for flood peak prediction is unattainable given the large number of variables, the uncertainty in flood level predictions should be communicated as well.

Water level prediction for the river Rhine at Lobith have been developed since 1982 (Sprokkedreef, 2001). Initially, predictions with a two day lead time were based on a multiple linear regression (MLR) model called LobithW. Longer lead times gave results that were too unreliable for practical purposes. LobithW used upstream water levels and rainfall predictions as independent variables and predicted water levels at Lobith, the gauging station at the Dutch-German border. In a number of steps the LobithW model was refined for different discharge levels, but the results did not meet the requirements of a prediction accuracy better then 10, 15, 20, and 40 cm for the one, two, three and four day lead time, respectively. Additionally, landscaping measures implemented to reduce flood levels would also render the MLR equations less reliable (Sprokkedreef, 2001).

To overcome the limitations of LobithW, a physically based model was set up called FloRIJN, which has been operational since 1999. It consists of a rainfall runoff model, HBV-96 (Lindström et al., 1997) coupled to a 1D hydrodynamic model, Sobek-RE. This model cascade is run in historic mode to reproduce the correct model state at the onset of the forecast. Next, the model is run in forecast mode to give water levels and discharges with a 1 to 4 day lead time (Sprokkedreef, 2001). This deterministic model provided improved forecast accuracies for the 3 and 4 day prediction, but for the 1 day prediction, the MLR model was still better. In the operational setting FloRIJN and LobithW ran parallel, and an experienced operator decided which values were published online to eliminate large outliers (Sprokkedreef, 2001).

Recently data assimilation tools and ensemble Kalman filtering have been developed to further increase the forecasting accuracy and to accompany the forecast with an estimate of the uncertainty (Reggiani and Weerts, 2008; Reggiani et al., 2009). Based on weather forecast ensembles multiple hydrological forecasts are made, giving a spread in the forecasted discharge and water levels over a 2-10 day period depending of the weather forecast used (Weerts, 2008). This is a computationally intensive method, that can be run once a day without major investments in computing power. In the Netherlands, this is implemented in the Delft-FEWS interactive data platform. Data assimilation and ensemble Kalman filtering are implemented in DAtools, a generic data assimilation tool (Weerts et al., 2010).

To overcome the computational cost of the ensemble Kalman filtering, Sumihar et al. (2009) implemented quantile regression. In quantile regression, the variation in the predicted water levels of the forecast is represented by quantiles, which are based on the predicted discharge. In this methodology, uncertainty estimates at any location in the model domain are based on the historic performance of forecasts and do not require the computational effort that would be needed for uncertainty bounds based on multiple forecasts. The drawback of quantile regression is the long time serie that is required to estimate the quantiles reliably. These time series are also affected by mitigating measures taken to lower the flood levels, lowering the quantile estimates.

In operational flood forecasting most efforts have been directed towards the accurate prediction of the river discharge by parameterizing the rainfall-runoff relation and the inflow of smaller catchments. The routing of the water through the 1D model is not considered a significant source of error. For example, Reggiani and Weerts (2008) consider the flow model well calibrated for the purpose of real time flood forecasting for the river Rhine. However for floods with the magnitude of the design discharge the water levels will rise above calibration levels and that may introduce errors due to extrapolation beyond the historic water levels. The uncertainty due to this extrapolation error is not known. These errors would not show up in flood predictions of an event with a two year return period or less, such as used by Reggiani et al (2009] and Weerts (, 2008 #83), as these events are of a lower magnitude than the event used for model calibration. The key contributors to the extrapolation error are the hydrodynamic roughness values (or “friction parameters”) of the main channel and the floodplains, as these are the parameters that are adjusted to achieve calibration of the model to historical flow events.

Uncertainty in friction parameterization has been quantified by Straatsma and Huthoff (2011) for floodplain friction parameterization and Warmink et al. (submitted) for the combined effect of floodplain and main channel parameterization. Straatsma and Huthoff (2011) showed that, regarding floodplain roughness, the land cover classification accuracy contributes most to uncertainty in predicted flood water levels. They showed that a 69% classification accuracy of the floodplain landcover leads to a 27 cm uncertainty (68% confidence interval) in water levels for the Rhine branches in The Netherlands. Other error sources related to the floodplain roughness parameterization appeared to be less relevant. (Straatsma and Huthoff, 2010) showed the inverse relationship between classification accuracy and model uncertainty. At a 95% classification accuracy, the 68% confidence interval reduces to 13 cm uncertainty in water levels. Warmink et al. (submitted) showed that the 95% confidence interval for the combined effect of uncertainty in friction parameterization of channels and floodplain together was 70 cm for the river Waal. These uncertainty values represent the uncertainty at the design discharge without taking into account the uncertainty-reducing effect of model calibration. For example, if the highest discharge event that is used for calibration was very close to the extrapolated design discharge, then naturally the extrapolation error would be small, because at the near-by calibration discharge the model “guarantees” a close to perfect water level prediction. At discharges that are further beyond the highest calibration discharge, the level of certainty of the water level prediction depends on the quality of the represented flow domain and on the proper interaction with water flowing through the domain. For the Dutch Rhine branches, calibration was carried out using flood peak of 1995 with a peak discharge of 12000 m<sup>3</sup>/s at Lobith, while the design discharge is 16000 m<sup>3</sup>/s. Hence a 4000 m<sup>3</sup>/s extrapolation is applied. The error due to this extrapolation is unknown.

The extrapolation error due to uncertain floodplain roughness parameterization not only relates to the determination of the design water levels, but also to the uncertainty in the operational flood forecasting. In operational flood forecasting the desired accuracy for water level predictions at Lobith during high water are 10, 15, 20, and 40 cm for the forecasts with a one, two, three, and four day lead time, respectively (Sprokkedreef, 2001). A number of studies have been carried out to assess the prediction uncertainty all related to a few flood peaks (Sprokkedreef, 2001; Reggiani and Weerts, 2008; Weerts, 2008). No study has presented an overview of the prediction uncertainty over a longer period of time.

Therefore the objectives of this study are to:

- > Determine the effect of model calibration on the uncertainty of the water levels at design discharge due to errors in floodplain friction parameterization.
- > Make the link to operational flood forecasting.

To reach the first objective, we created 15 roughness input files based on the landcover map and its classification error matrix. We subsequently ran the 2D WAQUA model of the Rhine branches at nine stationary discharges and quantified the extrapolation error for different extrapolation intervals. For the second objective, we carried out an assessment of the prediction error for flood peaks in the period between 2001 and 2011. In addition, we assessed the uncertainty in operational flood forecasting by hindcasting the 2003 flood peak using a 1D flow model with 15 different roughness patterns.

This is a follow up study of the FC2015 projects reported by Straatsma and Alkema (2009), and Straatsma and Huthoff (2010). This research, **deliverable 2011.06.04.1**, was carried out within the Flood Control 2015 program. For more information please visit <http://www.floodcontrol2015.com>.



## 2 FLOODPLAIN ROUGHNESS

### 2.1 UNCERTAINTY IN FLOODPLAIN ROUGHNESS

Roughness determines the retardance of the water flow. The higher the roughness, the slower the water will flow and, hence, the higher the water levels will reach. For the non-vegetated river bed, the roughness depends on the grain size and bed form dimensions (Van Rijn, 1994). Vegetation roughness of the floodplains has been described by many different models (Petryk and Bosmajian, 1975; Kouwen and Li, 1980; Kouwen, 2000; Baptist et al., 2007; Huthoff et al., 2007). It depends on vegetation structural characteristics like vegetation height and density, rigidity of the stems and the presence of leaves. Vegetation density is defined as the sum of the projected plant areas in side view per unit volume ( $m^2m^{-3}$ , which reduces to  $m^{-1}$ ). Seasonal variation and management that allows vegetation to vary dynamically lead to a high spatiotemporal variation of vegetation structural characteristics and inherent roughness patterns (Baptist et al., 2004; Jesse, 2004; Van Stokkom et al., 2005).

Uncertainty in the parameterization of floodplain roughness consists of four main factors: (1) classification accuracy of the landcover, (2) accuracy of the vegetation structural characteristics that link the landcover to input for roughness models, (3) the scale at which the landcover map has been generated, and (4) the choice of the roughness model that computes the roughness based on vegetation parameters, and hydrodynamic conditions.

Uncertainty in hydrodynamics resulting from error sources 1 to 3 were quantified by Straatsma and Huthoff (2010; 2011) in a previous FC2015 study using a 2D hydrodynamic model. Based on 15 individual model runs with different realizations of the roughness maps, the 68% confidence interval, also called spread, was computed at each riverkilometer in the Rhine branches.

Figure 1 shows the spread for all distributaries together as a boxplot of the spreads at all river kilometers together. This graph clearly shows that classification accuracy is the dominant source of uncertainty in water levels. Even at a 95 % classification accuracy, the uncertainty due to classification error is larger than the within class variation and the scale error.

These results are in the same order of magnitude as the results from the sensitivity analysis carried out by Stolker et al. (1999). They modeled differences in water level using a 1D model. Assuming floodplains covered with meadows, the land cover was varied over a length of 10 km with different vegetation types and a cover percentage varying between 10 % and 100 %. For example, in case 10 % of the land cover in the floodplain is changed from meadow to reed over a 10 km stretch of river, the peak increase in water level is 15 cm. Similarly, Huthoff and Augustijn (2004) report an 8 cm change in water level and stress the effect of the shape of the cross section of the river.

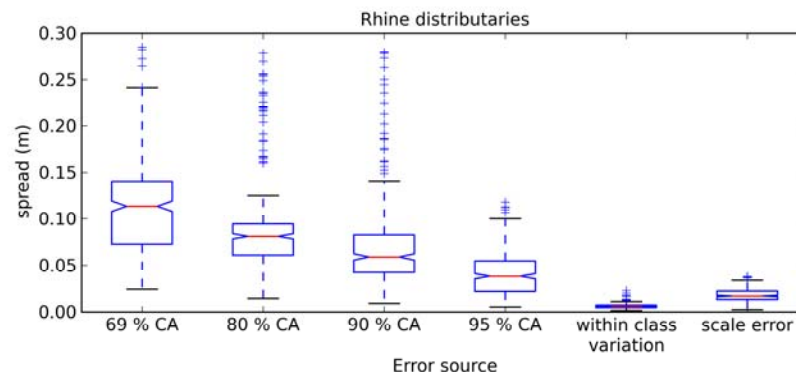


**Figure 1: Comparison between uncertainty due to different error sources of floodplain vegetation. Classification error is the dominant source of uncertainty. Even at the 95 % classification accuracy at ecotope group level. The effect of calibration is not included in this graph.**

The effect of the choice of the roughness model was investigated by (Warmink et al., submitted). They compared four roughness models that were developed for rigid vegetation, i.e. Klopstra et al. (1997), Van Velzen et al. (2003), Baptist et al. (2007), and Huthoff et al. (2007). Each of these models computes the roughness based on vegetation characteristics like drag, and vegetation height and density, plus water depth.

All four roughness models have been validated using flume studies with relatively high flow velocities and low water depths unlike the situation in the dutch floodplains of the Rhine distributaries. All roughness models fit well to the flume data, but at higher water depths, roughness predictions differ significantly between the Baptist model on the one hand and the other three models on the other hand. For the river Waal, the differences in predicted water levels are up to 10 cm. Compared to the other three error sources presented in Fig. 1, the error due to the choice of the roughness model would rank between classification error and scale error. The overall ranking of uncertainty contribution is classification error > roughness model > scale error > within class variation.

## 2.2 ROUGHNESS PARAMETERIZATION IN WAQUA

The implementation of roughness in hydrodynamic models varies. For WAQUA, the required data for model input has been made available by the Ministry of Public Works, Transport and Water Management (RWS) in the Baseline 4.03 database (Hartman and Van den Braak, 2007). It contains a complete dataset of base maps, derived maps, and a model schematization for the Rhine branches. The hydrodynamic roughness is implemented in a very detailed form in the Baseline database. For WAQUA, hydrodynamic roughness is derived from point, line, and polygon information (Fig. 2).

Roughness polygons are derived from the ecotope map, which is combined with the outline of the main channel, lakes and high water free areas. All these maps are converted using a lookup table to determine the roughness-polygon map (Figure 2). Each roughness code for vegetation is linked to vegetation structural parameters, such as vegetation height and density plus bottom roughness and drag (Van Velzen et al., 2003). The roughness in the WAQUA model, expressed as Chézy C, depends on the water depth and is computed during runtime of the model using the equation presented in Klopstra et al. (1997). The roughness is assigned to the model computational cell and the energy loss is computed over the cell.

Point and line elements of roughness are derived from a database containing hedges, individual trees and tree-lined lanes. These files are compiled in the Digital Topographic Dataset of the wet infrastructure (DTB-nat). Hedges are parameterized as line elements, assigned with a height and a density, whereas single trees are represented as point data with tree diameter as relevant hydrodynamic parameter. The energy loss of these roughness elements is computed, and attributed to the cell boundary containing the roughness elements.

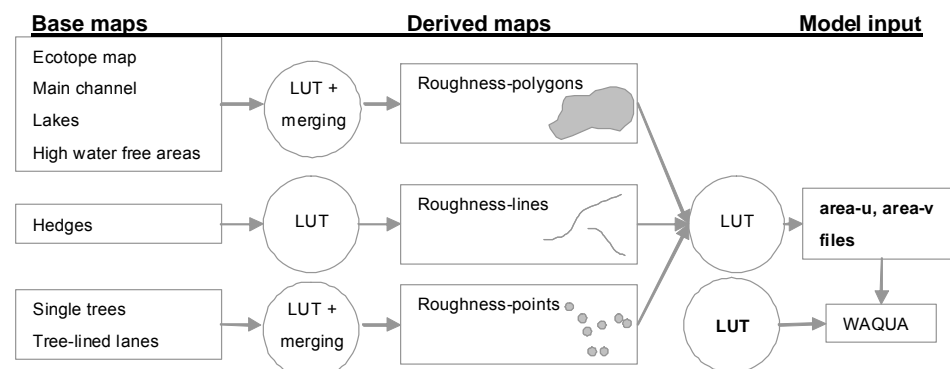


**Figure 2: Flow chart of roughness parameterization for the WAQUA hydrodynamic model. Only the ecotope map was varied in this study, which was varied according to the classification accuracy table (Knotters et al., 2008).**

The final model input to WAQUA consists of “area files” that describe the roughness in the downstream and the across stream direction (u and v). These files describe for each cell the fraction of the cell that is occupied with a specific roughness code, and the fraction of the cell that is covered by that roughness code. Another lookup table “rough.karak” links the roughness codes to vegetation parameters.

### 2.3 CLASSIFICATION ERROR IN ECOTOPE MAPS

Currently the vegetation map of the lower Rhine and Meuse floodplains is based on ecotopes. Ecotopes are 'spatial landscape units that are homogeneous as to vegetation structure, succession stage and the main abiotic factors that are relevant to plant growth' (Van der Molen et al., 2003). Mapping of ecotopes within the lower Rhine floodplain is based on visual interpretation and manual classification of vegetation units from aerial photographs, scale 1:10,000 (Jansen and Backx, 1998). Uncertainty in classification of the terrestrial ecotopes of the Rhine branches has been determined by Knotters et al. (2008) as map purities, the percentage of the mapped area that is correctly classified. The map purities table is similar to the confusion matrix, or error matrix, of a regular classification validation, except that the percentage of the total map that is correctly classified instead of the number of field reference points are listed in the cells. The map purities sum up to one per row. The map purity for the ecotope map of the Rhine branches of 2005 is estimated at 37% for 41 in the field distinguished different ecotopes ( $n=406$  field observations). The overall accuracy of this map is 69% when aggregated to eight terrestrial ecotope groups (Knotters and Brus, conditionally accepted). Classification accuracy is the number of correctly classified points divided by the total number of points in a regular classification. For the map purity table, it is the percentage of the map correctly classified divided by the total map area. In the map purity table (e.g. table 2) the classification accuracy is computed by the sum of the values on the diagonal divided by the sum of the the whole table.

To give an overview of the classification errors, we aggregated the map purity table to the vegetation types according to the vegetation handbook of Van Velzen et al. (2003) (Table 1). This was done by computing a weighted average over the lines of the ecotopes that are within the same vegetation class and summing up the columns that represent the same vegetation class. Weights were assigned based on the surface area of the ecotopes that were merged into a single vegetation type. Correct classifications are present in the diagonal of the map purity table, indicated in grey in table 1. Related to Fig. 3, an ecotope polygon representing production meadow would have a 52 % chance of keeping its vegetation type and a 48 % chance of being recoded to another vegetation type (Table 1).

A few problems were noted with the fieldwork related to the discernability of the different ecotopes in the field. Also, the spatial support of the field data (point measurements) did not match the aerial image interpretation of ecotopes per polygon, sized  $400 \text{ m}^2$  or more. Therefore the reported classification accuracy should be interpreted as a minimum value.

**Table 1 Map purity matrix in percentages for aggregated ecotopes in the Rhine branches (based on Knotters et al., (2008). Table should be read along the rows, e.g. agricultural area (fourth row) on the map was in correctly classified in 78.2%, and in 21.3% confused with production meadow according to the field validation. Also the total areas of the different ecotopes are given (ref km<sup>2</sup>: coverage of ecotopes in reference situation, after PM km<sup>2</sup>: coverage of ecotopes after application of the purity matrix, dA: change in surface area due to application of the purity matrix).**

Map representation	Roughness code	ref km <sup>2</sup>	after PM km <sup>2</sup>	dA km <sup>2</sup>	field reference data															
					Groyne field / sand bar	Builtup area / paved	Agricultural area	Pioneer vegetation	Production meadow	Natural grass/hayland	Dry herbaceous veg.	Reed-grass	Reed	Softwood shrubs	Willow plantation	Thorny shrubs	Softwood production forest	Hardwood forest	Softwood forest	
					111	114	121	1250	1201	1202	1212	1804	1807	1231	1232	1233	1242	1244	1245	
<b>Equivalent roughness length<sup>a</sup></b>																				
Groyne field / sand bar	111	3.4	4.1	+0.7	85.7															
Stone protection	113	0.5	0.0	-0.5		80.0									20.0					
Builtup area / paved	114	13.8	18.2	+4.4		91.6			4.9					1.7			1.7			
Agricultural area	121	35.3	32.9	-2.5			78.2		21.3	0.3	0.2									
<b>Submerged vegetation (grass-type)</b>																				
Pioneer vegetation	1250	0.8	2.5	+1.7	53.1	24.4		7.6		15.0										
Production meadow	1201	135.4	102.8	-32.6	0.5		2.2		51.7	32.5	6.7			3.1				2.9		
Natural grass/hayland	1202	71.8	77.8	+6.0		0.7	2.5	2.2	33.3	43.1	7.7	2.7	5.5					2.3		
<b>Submerged vegetation (reed-type)</b>																				
Dry herbaceous veg.	1212	22.4	29.9	+7.5		9.9	2.3	4.3	1.7	7.6	52.8	3.9	2.2	5.2	4.6	4.3	1.8			
Reed-grass	1804	3.7	3.7	0.0						22.0	58.9			16.0						3.0
Reed	1807	3.4	6.8	+3.4								26.3	64.7	9.0						
<b>Emergent vegetation</b>																				
Softwood shrubs	1231	4.0	11.1	+7.1		0.4			3.0	3.0	10.1		3.0	43.3		12.1	16.0	0.8	8.3	
Willow plantation	1232	0.1	1.0	+1.0																100
Thorny shrubs	1233	1.6	2.3	+0.7		9.2				5.4	15.8			19.6		21.4	2.0	10.5	16.2	
Softwood product. forest	1242	2.6	8.7	+6.2		12.0			6.0					0.4		7.8	43.2		30.7	
Hardwood forest	1244	5.9	2.1	-3.8		29.8								11.7			11.6	31.8	15.2	
Softwood forest	1245	11.2	12.0	+0.8							5.9			11.3		3.3				79.4

<sup>a</sup> “Groyne field / sand bar” refers to the roughness of the area between the groynes along the main channel, or sandbars in side channels, “stone protection” is the roughness code for shorelines that are protected with rubble, “built up areas / paved” is a single class for the roughness of hard surfaces, “agricultural area” refers to the roughness of fields.



### 3 STUDY AREA

Within this study, we looked at the distributaries of the river Rhine in the Netherlands, excluding the estuary. At the Dutch-German border, the river Rhine has an average discharge of 2250 m<sup>3</sup>/s, draining a catchment area of 165 000 km<sup>2</sup>. Coming from Germany, the river Rhine bifurcates into the "Pannerdensch Kanaal" and the Waal river at the "Pannerdensch Kop" (PK) bifurcation point where roughly one third enters the "Pannerdensch Kanaal" and two thirds are conveyed into the river Waal. At the "IJsselkop" (IJK) bifurcation points again, one third enters the right hand channel named the IJssel river and two thirds flow into the Nederrijn river (Fig. 2). However the exact ratio of dividing the water over the channels depends on the shape and roughness of the main channel and the floodplain.

The study area spans three distributaries with an average water gradient of 0.10 m/km and a maximum length of 152 km along the river axis, which is for the IJssel. The total embanked area amounts to 440 km<sup>2</sup>, the floodplain area is 320 km<sup>2</sup> out of which 48 km<sup>2</sup> consists of lakes and side channels. The vegetated area takes up 62 % of the total embanked area. Groynes fixate the main channel and limit the width of the main channel to 250, 160, 105 m for the Waal, Nederrijn and IJssel river. The cross-sectional width between the primary embankments varies between 0.5 and 2.6 km. Meadows dominate the land cover, but recent nature rehabilitation programs led to increased areas with herbaceous vegetation, shrubs and forest.

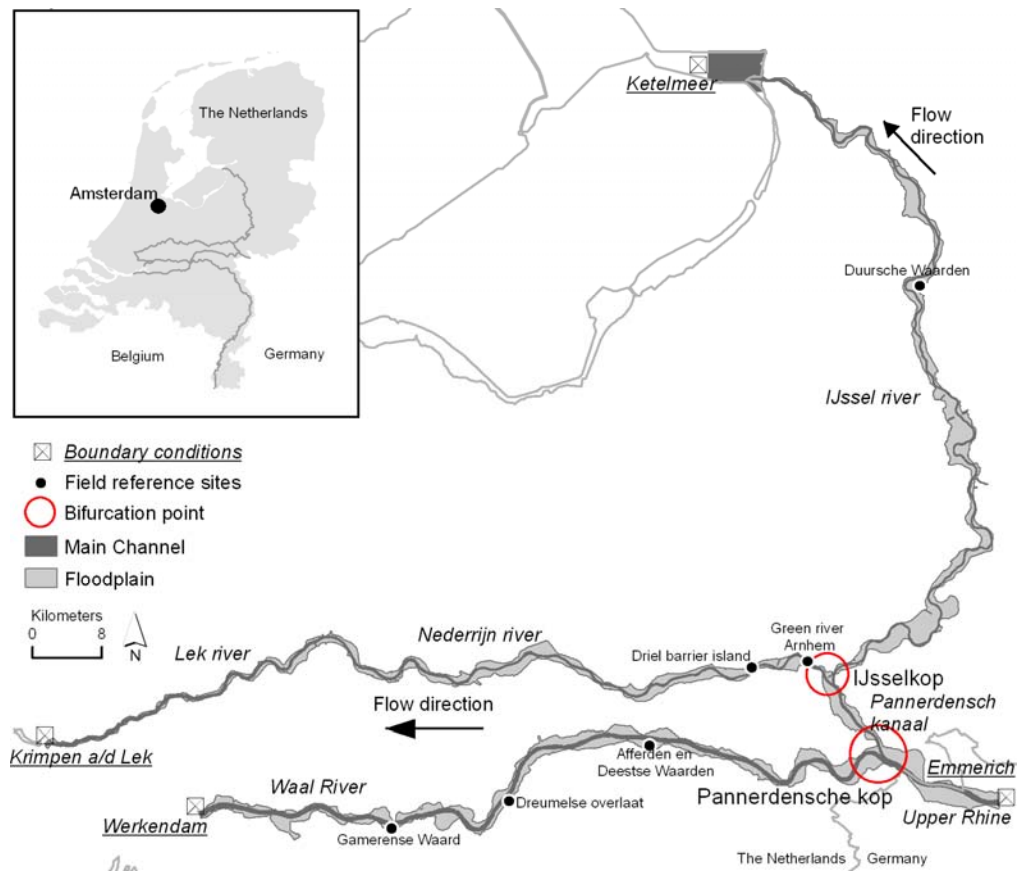


**Figure 3** Study area showing the three main distributaries of the river Rhine; Waal, Nederrijn/Lek and IJssel river. At the bifurcation points "Pannerdensch Kop" and "IJsselkop" the water is distributed over the three branches.



## 4 METHODS

In this study, we focused on the quantification of the extrapolation error due to uncertainties in floodplain roughness parameterization using the WAQUA hydrodynamic model. Firstly we created 15 new ecotope maps at a classification accuracy of 69% at ecotope group level, plus 15 new realizations at 95% classification accuracy. These maps were subsequently converted to WAQUA model input. WAQUA was subsequently run at nine stationary discharges. The uncertainty was determined by the variation in roughness, flow velocities, water levels and discharge distribution.

### 4.1 NEW REALIZATIONS OF ECOTOPE MAPS

#### *Ecotope map preprocessing*

The first step consisted of matching the coding of the latest ecotope map with the coding used in the field validation. The map purity table of Knotters et al. (2008) has been standardized by Straatsma and Alkema (2009). This matrix is presented in Appendix 1. Both the field validation and the adjusted map purity matrix are based on the second cycle of the ecotope mapping, which was carried out in 2005. However, the most recent ecotope map that is being used for hydrodynamic modeling is a revised version of the second ecotope cycle. The revision included recoding of ecotope names to highlight the tidal influences in the downstream parts of the distributaries plus a number of compound classes were defined to better describe the combinations of ecotopes at a specific location. These new ecotope codes were not taken into account in the validation. Hence, there is no map purity table that includes these ecotopes. To be able to assign new ecotope codes for the 15 realizations, we recoded the revised ecotope map of the second mapping cycle to the codes existing in the unrevised version of the ecotope map of the second cycle. This gave a simplification of the final error matrix as less classes were used.

The surface area of the ecotopes that needed recoding totalled 70 km<sup>2</sup> out of the total of 523 km<sup>2</sup> of the ecotope map. Only 15 km<sup>2</sup> consisted of terrestrial ecotopes. The recoding of ecotopes is presented in Table 2 and involved expert judgment by two ecologists. For the water ecotopes, we chose a new code that did not alter the resulting roughness. Some ecotopes were only renamed in the revision, such as “REST-O-U” to “O-U-REST,” the codes for temporarily bare floodplains, or natural levees. The result of was a complete map purity table covering all the ecotope classes in the ecotope map.

Nonetheless, the recoding affected the assignment of new ecotope classes for the 15 new realizations as these are determined by the map purity table. For example, the compound class “VI.4/HB-1” of the revised map consists of both softwood forest, coded as “VI.4”, and highwater free natural forest, coded as “HB-1.” This compound class was recoded to natural floodplain forest, coded as “UB-1,” because it is a class that is both natural and not so often inundated. This means that “UB-1” will be used to generate new realizations of this polygon. The result would differ if “HB-1,” or “VI-4” was used. Given the small surface area of the recoded polygons, we assume that the influence on hydrodynamics is negligible. This problem could only be solved by linking the ecotope map to a complete field validation, which is outside the scope of this research.

#### *Generating new realization of the ecotope maps*

The method to create new realizations of the roughness maps has been presented in Straatsma and Huthoff (2011) and will be iterated here in brief. We used the map purities table (Table 2) as probabilities that an ecotope polygon is classified correctly. We computed the cumulative probability by summing up the probabilities along each row in the map purities table (Fig. 4). For each polygon in the ecotope map, we drew a random number between zero and one with a uniform distribution, and using the cumulative probability we assigned a new ecotope code to each of the polygons (Fig. 3). This procedure was repeated 15 times for each polygon in the original map, giving 15 new realizations of the ecotope map. Each has the same probability and can be seen as different outcomes of the same manual procedure of creating the ecotope map. These maps were recoded to WAQUA roughness files using the Baseline software (Hartman and Van den Braak, 2007).

**Table 2 Recoding of new ecotope in the revised second cycle of the ecotope map to the original second cycle of the ecotope map.**

<b>New codes in revision</b>	<b>Description</b>	<b>Recoded to</b>	<b>Description</b>
VI.5-6/HB-1	High water free, or rarely inundated floodplain, or natural forest	HB-1	Natural forest
VI.6	Rarely inundated floodplain forest	HB-1	Natural forest
HM-1-2	Reed	HM-1	Reeds and other helophytes
I.1/MzO-M-D-Z	Dynamic sweet to brackish shallow water, or sandy shallow lake	I.1	Shallow water
I.5	Low dynamic sweet to brackish shallow water	I.1	Shallow water
II.2-3	Sweet sandy, or silty sand bars	II.2	Bare river bar
III.2-3/HA-2	Hard substrate with medium to high dynamics influenced by sweet water, not bare	III.2-3	Paved / Builtup area
IV.1	Species poor helophytes in shallow water	IV.8-9	Reeds and other helophytes
IV.1-2-6-8	Helophytes in shallow water, helophyte culture, or species poor helophyte swamp	IV.8-9	Reeds and other helophytes
IV.11	Reed	IV.8-9	Reeds and other helophytes
IV.3	Sweet water bulrush	IV.8-9	Reeds and other helophytes
REST-O	Natural levee, temporarily bare	O-U-REST	Rest
REST-O-U	Natural levee, or floodplain, temporarily bare	O-U-REST	Rest
REST-T	Temporarily bare	REST	Rest
RnD	Deep side channel	RnD	Rest
RnO	Shallow side channel	RnM	Side channel
RwX	River accompanying water	RwM	River accompanying water
VI.4/HB-1	Floodplain forest, or high water free natural forest	UB-1	Natural forest
REST-U	Floodplain temporarily bare	U-REST	Rest
V.1-2-3-4	Species poor, or rich swamp, or bulrush	V.1-2	Herbaceous vegetation
V.2	Species poor swamp	V.1-2	Herbaceous vegetation
VI.1	Grey willow shrub	VI.2-3	Shrubs
VI.1/HB-2	Grey willow shrub, high water free shrub	VI.2-3	Shrubs
VI.2	Softwood shrubs	VI.2-3	Shrubs
VI.2/HB-2	Softwood shrub, high water free shrub	VI.2-3	Shrubs
VI.5	Flood forest	VI.4	Natural forest
VII.1-2	Grass land: swampy flooding, or stucture rich	VII.1	Natural grassland
VII.1-2-3	Grass land: swampy flooding, or stucture rich, or production meadow	VII.1	Natural grassland
VII.1-2-3/HG-1-2	Grass land: swampy flooding, or stucture rich, or production meadow, possibly high water free	VII.3	Production meadow
VII.3/HG-2	Production meadow, possibly high water free	VII.3	Production meadow

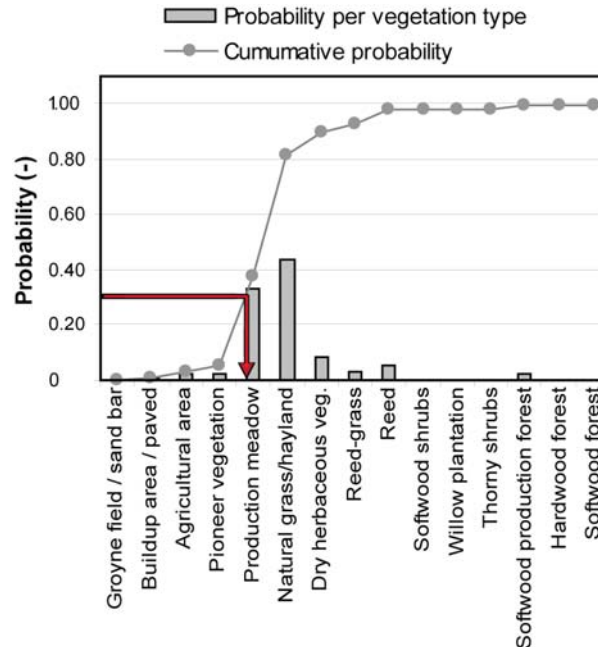


**Figure 4 Recoding based on the cumulative probability function derived from the map purities. map purities are for a meadow polygon. The red arrow gives the random number of for a meadow (0.81) and the subsequent recoding into herbaceous vegetation as the random number is between 0.6 and 0.95.**

The validation of the ecotope map was disputed due to the difference in support between field data and aerial image interpretation and some of the ecotope types were not discernable from one another based on the plant communities. Therefore the true accuracy of the ecotope type is not known. The reported accuracy is assumed to be a minimum, given the classification accuracies reported in other studies that vary between 70 % and 92 % (Van der Sande et al., 2003; Geerling et al., 2007; Straatsma and Baptist, 2008).

In anticipation of a future undisputed validation of the ecotope map, we wanted to establish the extrapolation error at two levels of classification accuracy of the ecotope map: the current 69 % accuracy at ecotope level, and a possible future 95 % classification accuracy at ecotope group level.

To determine the uncertainty in water levels, we created a new map purity tables that represent the classification accuracy at ecotope group level of 95% based on the current table that has a 69% classification accuracy. The new map purity table was created by increasing the values on the diagonal and decreasing the values off-diagonal in the map purity table using the following method. The off diagonal values were decreased by a manually chosen multiplication factor between 0 and 1. For each line in the matrix, the difference between the original off-diagonal values and the new values was added to the diagonal value. This led to the increase in the diagonal value and decrease of the off-diagonal values, leading to a new error matrix with a higher classification accuracy. The ecotope map purity matrix was subsequently aggregated into 8 ecotope group classes and 16 vegetation type classes. The multiplication factor was changed by trial and error until the classification accuracy at ecotope group level reached 95% (Table 3).

**Table 3 Characteristics of classification accuracies.**

Set	Classification accuracy at ecotope group level	Classification accuracy at vegetation type level
1	69 %	43 %
2	95 %	92 %

At each accuracy level 15 new realizations were created of the ecotope map totalling 30 ecotope maps. The 15 random numbers were drawn once for each polygon. These 15 random numbers were used to generate 15 realizations at 69% CA as well as at 95% CA. Thereby making sure that the resulting uncertainty in the hydrodynamics only reflected the change in classification accuracy and not a difference due to drawing new random numbers for each of the two sets of maps.

## 4.2 HYDRODYNAMIC MODELING

### *WAQUA hydrodynamic model*

The WAQUA model has been used by the Dutch Ministry of Transport, Public Works and Water Management for the two-dimensional simulation of hydrodynamics in the complex channel and floodplain areas of the Rivers Rhine and Meuse in the Netherlands (RWS, 2007). For the present study, a series of simulations of steady flow in the study area was carried out. The WAQUA model that was used for this study is based on a staggered curvilinear grid. Each of the 886,861 cells represents a column shaped volume of water with a variable surface area of 700 m<sup>2</sup> on average. The water flow between the water volumes in the raster is calculated by numerically solving the Saint-Venant equations of mass balance and of convective and diffusive motion in two dimensions (RWS, 2007) using a finite difference method. The boundary conditions of the model are the river discharge at the upstream boundary, and the water level at the downstream boundary using a rating curve. Input data from which the WAQUA model calculates the water flow field are a Digital Terrain Model (DTM), barriers and a roughness map. Optional information may be provided on the operation of weirs and lateral inflow.

### *Simulations*

To be able to determine the extrapolation error, we ran WAQUA with a series of stationary discharges applied to the upstream boundary at Emmerich, Germany. Downstream water levels were governed by a rating curve for each distributary. Nine different discharge levels were applied: 3500, 4000, 5000, 6000, 7000, 8000, 10000, 12000, and 16000 m<sup>3</sup>/s. The lowest discharge will give the first inundation of the floodplains. The highest discharge refers to the design discharge with a statistical return period of 1250 years. A discharge of 10000 m<sup>3</sup>/s is the normal high water with a return period of 10 years, the 12000 m<sup>3</sup>/s flow rate corresponds to the historical event of 1995 that is still used for model calibration. In total 270 model runs were carried out (2 accuracy levels times 9 discharge levels times 15 roughness realizations). Initial condition of water level and flow velocities were determined by running the model for 10 days at each of the discharge levels. The simulation time for the runs was set to three days to stabilize the water levels and discharge distribution. The full model of the Rhine branches was run as proximity of the boundaries to the bifurcation points would limit the effect of water level variations. Output of the computations consisted of spatially distributed values of the Nikuradse equivalent roughness length, flow velocities, water levels, and the discharge distribution over the bifurcation points.

### *Extrapolation error*

Uncertainty in model predictions is reduced by adjusting the roughness values of the main channel in The Netherlands. Other methods will change both the roughness of the main channel and of the floodplain to make the model predictions match field observations, or remote sensing derived flood extent maps (Schumann et al., 2009). This limits the uncertainty in the predictions and gives the model error after calibration. Subsequently, the models often are run at higher discharges and no information is available on the error after extrapolation.

In this research, we computed the extrapolation error for each interval between the nine different discharge levels using the following steps:

- > Run the WAQUA 2D model of the Rhine distributaries at nine stationary discharges for 15 realizations of the ecotope maps at 69% classification error, yielding a total of 135 model runs.
- > Extract the water levels at the river axis for each of the 135 model runs. This will give the uncertainty in water levels as a function of river discharge, but without error reduction due to calibration.
- > Compute the discharge for each of the distributaries and each of the 135 runs. Summarize by the spread per distributary and discharge level.
- > Compute the differences in water levels for each of the intervals between the nine discharge levels. Thereby, we assumed that the water levels are perfectly described after calibration by each discharge level, because we only looked at the *differences* between the water levels.
- > Determine the minimum, maximum, 16<sup>th</sup> and 84<sup>th</sup> percentile, and 68% confidence interval (spread) of the water level differences at each river kilometer and extrapolation interval.
- > Summarize the statistics of the spread for each distributary, i.e. Bovenrijn-Waal, Pannderdensch Kanaal-Nederrijn-Lek, and IJssel. Visualize as box plots for extrapolation to the design discharge and as line graphs for all discharges.
- > Repeat for the 95% classification accuracy.

In appendix 6 the practical procedure to quantify the extrapolation error is explained in further detail, together with an analysis that suggest the use of a correction factor *f* to be included when calculating this extrapolation

error. The suggested value of the correction value for the Rhine branches is around  $f = 0.3$ , but this value requires further research. Therefore, in the current work we adopt no correction (i.e. correction factor  $f = 1$ ), which gives a conservative estimate of the resulting extrapolation error (i.e. a maximum extrapolation error).

#### *Speed of rise of discharge during flood peaks*

The speed of rise during the flood peak also influences the extrapolation error. During a steep peak, the difference in the discharge from one day to the next will be more than during a broad flood hydrograph. Hence, also the extrapolation error will be more during a steep peak. To get an idea of the distribution of the rise in discharge over a one to four day period during a flood peak, we assessed the complete recorded discharge data serie of Lobith spanning the period between 1901 and 2007. Therefore we analysed the speed of rise of all the flood peaks since 1901 with a peak of more than  $5000 \text{ m}^3/\text{s}$ .

### **4.3 PREDICTION UNCERTAINTY IN OPERATIONAL FLOOD FORECASTING**

To get a systematic overview of the prediction uncertainty in operational flood forecasting, we assessed all flood peaks from 2001 to 2011, the period that four day forecasts are available. Initially, FloRIJN was available as a physics based flood model. Since 2010, Delft-FEWS has been used operationally in the flood forecasts. However, during high water the predictions that are sent out to the public are corrected by a group of specialists on peak flood forecasting of the Ministry of Infrastructure and Environment. These published values are based on the predictions of all three models, and are supposed to filter out extreme prediction errors.

We analysed the published predictions for all flood events between April 2001, and February 2011. The results were summarized in a figure and table listing the Mean Absolute Error (MAE) for the 1-4 day forecasts. The MAE was computed based on the days the measured water levels exceeded 12 m at Lobith. The MAEs were compared to the desired accuracy levels for the one to four day lead times.

## 5 RESULTS

The methods that we used to substantiate the objectives with data are presented in this chapter. First we will present the output and subsequent analysis of the hydrodynamic modeling. Then we present the results of the accuracy assessment of the current operational flood forecasting.

### 5.1 UNCERTAINTY IN HYDRODYNAMICS RELATIVE TO FLOW RATE

To be able to contrast the results of the extrapolation error, we first present the uncertainties in hydrodynamics at the nine different flow rates. We will present water levels in the three different distributaries and the discharge distribution over the bifurcation points.

#### 5.1.1 Water levels

Water levels vary due to the different realizations of the floodplain friction. We show the effect of the different ecotope maps on the water levels at the river axes of the distributaries. Figure 5 gives the outcome of the individual runs as thin grey lines. It represents the variation in water levels for the river IJssel due to 69% classification accuracy. The blue lines indicate the 16<sup>th</sup> and 84<sup>th</sup> percentiles, and the 68% confidence interval is shown as a red line. The 1D results for the Bovenrijn-Waal, and the Pannerdensch Kanaal-Nederrijn-Lek are given in Appendix 3, which includes the results for the 95% classification accuracy. The zero level in these graphs represents the average predicted water level at that river kilometer. For each run, the deviation from this average has been depicted to optimize interpretation of the results.

It is clear from figure 5 that the spread in the water level correlates positively with discharge. At a discharge of 3500 m<sup>3</sup>/s, the floodplains convey little water, hence the differences in roughness have only a small effect on the water levels at the river axis. Up to a stationary discharge at Lobith of 7000 m<sup>3</sup>/s the spread in water level is limited to less than 6.5 centimeter. At high discharges the floodplain roughness leads to a spread of 10 cm at 12000 m<sup>3</sup>/s, and of almost 20 cm at 16000 m<sup>3</sup>/s. At these discharges the fractional discharge over the floodplains is large, and the water levels are strongly influenced by the floodplain roughness. Individual floodplain sections may strongly affect the water levels. For example at river kilometer 905 and 925, a single realization of the floodplain friction is clearly generating outliers in the water levels at the river axis. The variations become more pronounced as the discharge increases. At 8000 m<sup>3</sup>/s the outliers generate a peak of 9 cm above average, while at 16000 m<sup>3</sup>/s the water levels are around 30 cm above average. In addition, additional peaks may show up at high discharges, such as the peak at river kilometer 885 at 16000 m<sup>3</sup>/s. This peak is completely absent at 12000 m<sup>3</sup>/s.

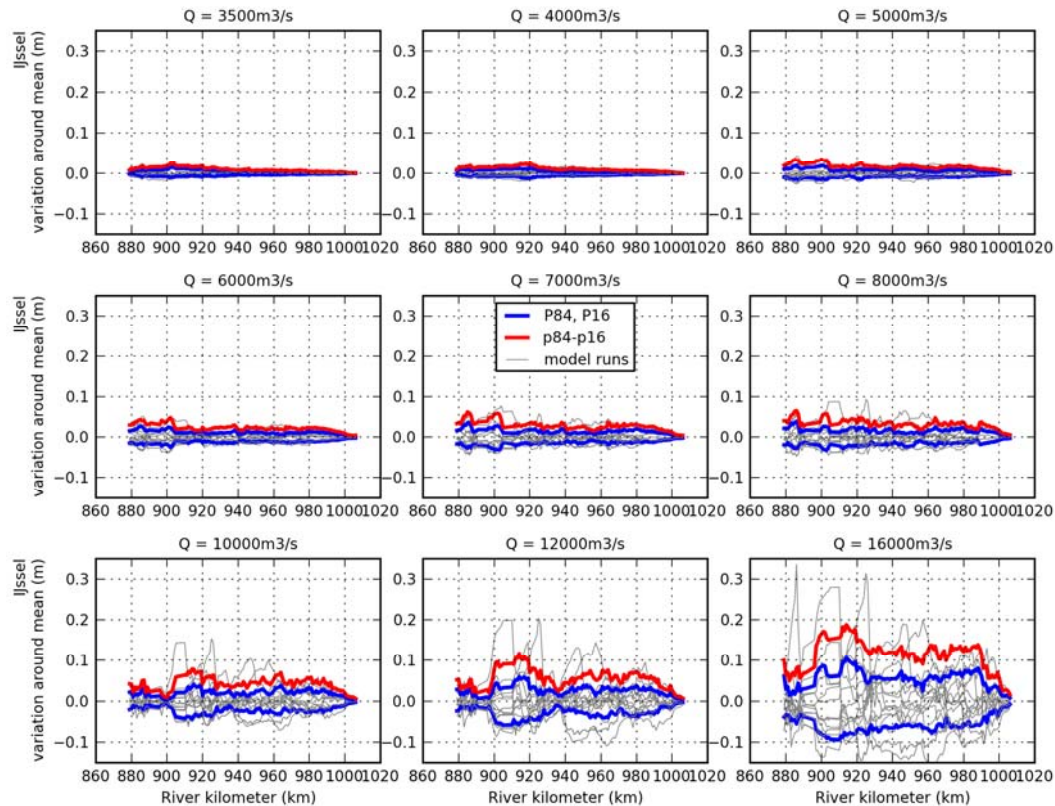


**Figure 5** Spread in water levels in the IJssel river due to a 69% classification accuracy for nine stationary discharges. The variation in water levels increases with the discharge.

The spread increases almost linearly as a function of discharge, both for the 69% as well as the 95% classification accuracy. Also the variation in the spread increases as a function of discharge. This is obscured in figure 8 by the larger increase in discharge at higher discharges, which suggests an exponential relationship. The spread for the 69% classification accuracy is two to three times as high as the spread due to the 95% classification accuracy. The flier points on the lower part of the distribution are caused by the downstream boundary conditions, where the rating curve limits the effect of the variation in roughness. The IJssel river generates the highest spreads, the Bovenrijn-Waal have the lowest spreads. Spreads of the IJssel are 50% higher than for the Waal (Figure 6 and Table 4). The reason is the high fractional discharge of the IJssel compared to the Waal.

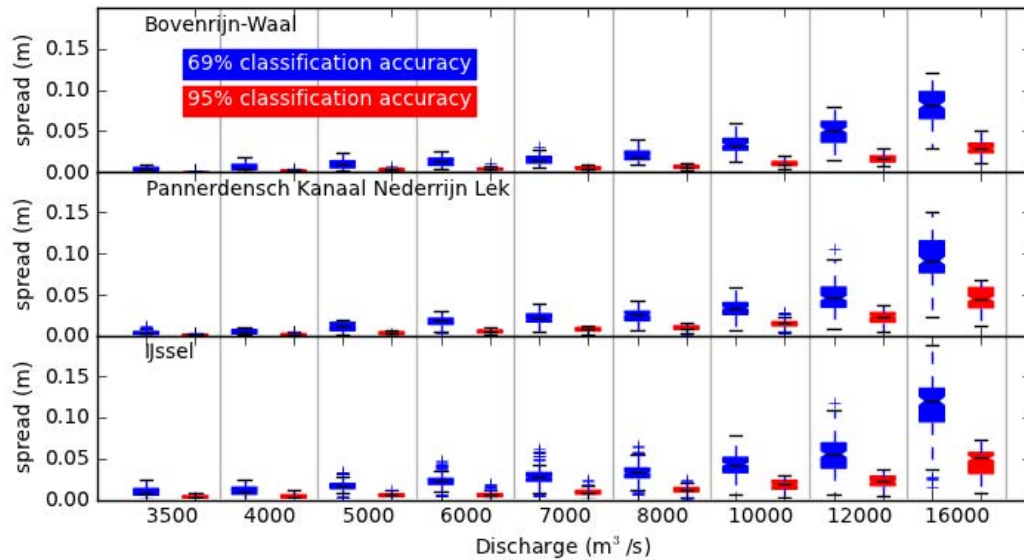


Figure 6 Distribution of the spreads in water levels for three distributaries at nine stationary discharges and two classification accuracies, i.e.69 and 95%. The blue boxes of the the lower panel are based on the same data as the red lines in Fig. 5. Other boxes are presented in Appendix 3. The median spread is given by the red line. The box represents the interquartile range, whiskers show the range of 1.5 times the interquartile range, and the flier points are the points beyond the whiskers.

Table 4 Overview of the uncertainty in water levels in the Rhine distributaries at 69 and 95% classification accuracy and nine discharge levels. The values represent the maximum spread and range in water levels between 15 model runs. In brackets the median value of the spread and range are given.

		Bovenrijn-Waal		Pannerdensch Kanaal- Nederrijn-Lek		IJssel	
Discharge (m <sup>3</sup> /s)		Spread (m)	Range (m)	Spread (m)	Range (m)	Spread (m)	Range (m)
69% classification accuracy	3500	0.01 (0.00)	0.02 (0.01)	0.01 (0.00)	0.02 (0.01)	0.02 (0.01)	0.04 (0.02)
	4000	0.02 (0.00)	0.03 (0.01)	0.01 (0.00)	0.03 (0.01)	0.02 (0.01)	0.05 (0.02)
	5000	0.02 (0.01)	0.04 (0.02)	0.02 (0.01)	0.04 (0.03)	0.03 (0.02)	0.07 (0.03)
	6000	0.03 (0.01)	0.05 (0.02)	0.03 (0.02)	0.06 (0.04)	0.05 (0.02)	0.09 (0.04)
	7000	0.03 (0.01)	0.07 (0.03)	0.04 (0.02)	0.07 (0.05)	0.06 (0.03)	0.11 (0.05)
	8000	0.04 (0.02)	0.08 (0.04)	0.04 (0.03)	0.09 (0.06)	0.07 (0.03)	0.13 (0.07)
	10000	0.06 (0.03)	0.14 (0.07)	0.06 (0.03)	0.10 (0.07)	0.08 (0.04)	0.20 (0.09)
	12000	0.08 (0.05)	0.21 (0.10)	0.11 (0.05)	0.20 (0.11)	0.12 (0.06)	0.28 (0.12)
	16000	0.12 (0.08)	0.30 (0.18)	0.15 (0.09)	0.36 (0.22)	0.19 (0.12)	0.44 (0.23)
95% classification accuracy	3500	0.00 (0.00)	0.01 (0.00)	0.00 (0.00)	0.01 (0.00)	0.01 (0.00)	0.01 (0.01)
	4000	0.00 (0.00)	0.01 (0.00)	0.01 (0.00)	0.01 (0.00)	0.01 (0.00)	0.03 (0.01)
	5000	0.01 (0.00)	0.01 (0.01)	0.01 (0.00)	0.01 (0.01)	0.01 (0.01)	0.02 (0.01)
	6000	0.01 (0.00)	0.02 (0.01)	0.01 (0.01)	0.02 (0.01)	0.02 (0.01)	0.04 (0.01)
	7000	0.01 (0.00)	0.03 (0.01)	0.01 (0.01)	0.04 (0.02)	0.02 (0.01)	0.04 (0.02)
	8000	0.01 (0.01)	0.03 (0.02)	0.02 (0.01)	0.05 (0.02)	0.03 (0.01)	0.05 (0.02)
	10000	0.02 (0.01)	0.04 (0.03)	0.03 (0.02)	0.08 (0.04)	0.03 (0.02)	0.08 (0.04)
	12000	0.03 (0.02)	0.06 (0.04)	0.04 (0.02)	0.10 (0.06)	0.04 (0.02)	0.11 (0.05)
	16000	0.05 (0.03)	0.10 (0.05)	0.07 (0.05)	0.16 (0.11)	0.07 (0.05)	0.22 (0.10)

### 5.1.2 Discharge distribution over the bifurcation points

The variation in roughness also influences the distribution of the water at the bifurcation points. Lower roughness leads to a lower water level locally which will increase the conveyance in that branche. The area directly downstream of the bifurcation points exerts the highest influence on the discharge distribution.

The spread in the discharge distribution increases with discharge, similar to the water level (Table 5). Due to a 69% classification accuracy the spread in the discharge for the Waal, at 10000 m<sup>3</sup>/s discharge level, is 30 m<sup>3</sup>/s, while at 16000 m<sup>3</sup>/s the spread is 89 m<sup>3</sup>/s. The spread in discharge due to a 69% classification accuracy is a factor 1.5 to 3 higher than the spread in discharge due to a 95% classification accuracy. These shifts in discharge may have a large effect on the water levels (Figure 7). A 200 m<sup>3</sup>/s increase in discharge raised the water levels with approximately 0.05 m at the model boundaries (Werkendam, Krimpen aan de Lek, Ketelmeer, Lobith; Figure 7;

Figure 3), but locally the increase may be as high as 0.25 m at the IJsselkop.

**Table 5** Spread in discharge distribution (p84-p16 percentile; m<sup>3</sup>/s) for the 69 and 95% classification accuracy and nine discharge levels. In brackets the range in discharge for each distributary. Statistics are based on 15 model runs.

	Discharge level (m <sup>3</sup> /s)	Spread Waal (m <sup>3</sup> /s)	Spread Pannerdensch Kanaal (m <sup>3</sup> /s)	Spread Nederrijn-Lek (m <sup>3</sup> /s)	Spread IJssel (m <sup>3</sup> /s)
<b>69% classification accuracy</b>	3500	1 ( 4)	1 ( 4)	1 ( 3)	1 ( 2)
	4000	2 ( 3)	1 ( 4)	1 ( 4)	1 ( 2)
	5000	4 ( 8)	4 ( 8)	4 ( 8)	4 ( 6)
	6000	9 ( 13)	8 ( 13)	8 ( 16)	8 ( 12)
	7000	15 ( 22)	15 ( 22)	10 ( 23)	11 ( 16)
	8000	25 ( 32)	25 ( 31)	18 ( 40)	15 ( 24)
	10000	30 ( 80)	30 ( 80)	27 ( 64)	24 ( 44)
	12000	40 (157)	42 (155)	37 (109)	35 ( 80)
	16000	89 (340)	85 (338)	95 (221)	65 (156)
<b>95% classification accuracy</b>	3500	1 ( 2)	1 ( 2)	1 ( 1)	0 ( 1)
	4000	0 ( 1)	1 ( 2)	1 ( 1)	1 ( 2)
	5000	1 ( 3)	1 ( 4)	1 ( 2)	1 ( 3)
	6000	1 ( 7)	2 ( 7)	2 ( 5)	2 ( 5)
	7000	2 ( 12)	3 ( 12)	4 ( 7)	4 ( 9)
	8000	5 ( 20)	5 ( 20)	6 ( 13)	6 ( 13)
	10000	9 ( 26)	10 ( 26)	14 ( 34)	12 ( 29)
	12000	24 ( 38)	23 ( 39)	25 ( 59)	18 ( 44)
	16000	58 ( 92)	49 ( 78)	50 (112)	37 ( 83)

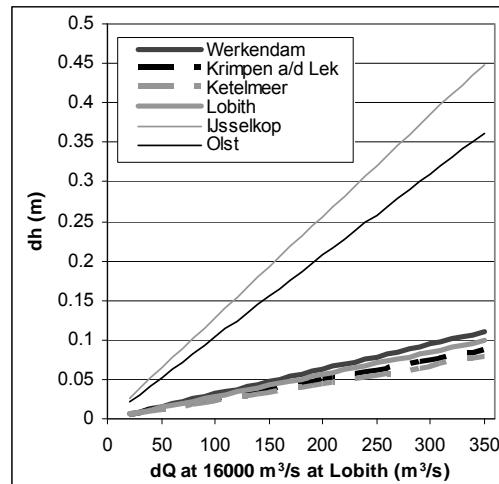


**Figure 7** Dependence of difference in water level on difference in discharge for four boundary water level stations in the Rhine distributaries (dQ-dh relationship at design discharge). Variation in discharge may due to changing roughness patterns around the bifurcation points may explain up to 0.10 m in water level.

## 5.2 EXTRAPOLATION ERROR

Similar to the uncertainty assessment, we will present the results on the extrapolation error with respect to water levels and discharge distribution. To see the relevance of the extrapolation error, we also present the results of the increase in discharge during flood peaks.

### 5.2.1 Water levels

The uncertainty in water level predictions due to errors in the floodplain roughness parameterization depends on the extrapolation interval (Figure 8). Figure 8 shows the difference in the water levels between the simulated calibration discharge and the design discharge of 16000 m<sup>3</sup>/s for the individual runs as grey lines. This is based on the predictions for the IJssel river and a classification accuracy of 69% at ecotope group level. For example, the top left panel gives the error when the model would be calibrated with a flood event of 3500 m<sup>3</sup>/s and then extrapolated to the design discharge of 16000 m<sup>3</sup>/s. This is quite hypothetical as this event has a very high return period and is not very representative of floodplain flow (Figure 5). This example is given for completeness.

It becomes clear that the variation decreases with the extrapolation interval. When a flood event of 4000 m<sup>3</sup>/s was used to calibrate the design discharge event (middle panel at the top) the maximum spread in extrapolation error is 19 cm at river kilometer 920 in the IJssel river. A calibration at 12000 m<sup>3</sup>/s would give a spread of the extrapolation error of 12 cm at river kilometer 900. For completeness the spread is also given for a calibration event of 16000 m<sup>3</sup>/s, which will give a spread of 0 cm as we assumed a perfect calibration. It suggests that a calibration at this discharge would result in zero uncertainty due to floodplain roughness parameterization, but it should be kept in mind that other error sources exist and that we worked with stationary discharges. The results for the Pannerdensch Kanaal-Nederrijn-Lek and the Bovenrijn-Waal show a similar pattern, both at 69% as well as at a 95% classification accuracy. These 1D results are all presented in appendix 3.

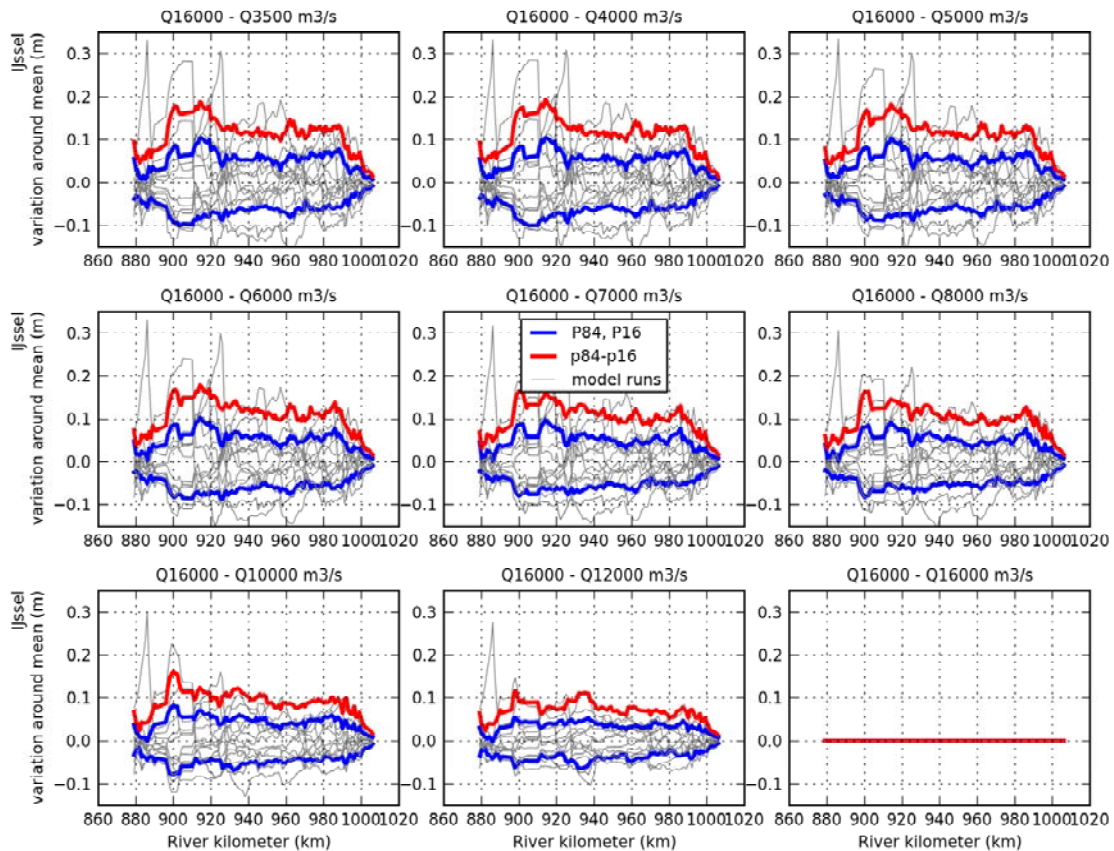


**Figure 8 Extrapolation error in the IJssel river for different discharges of calibration. The design discharge of 16000 m<sup>3</sup>/s is taken as the reference. The calibration discharge has been varied between 3500 and 12000 m<sup>3</sup>/s. At 16000 m<sup>3</sup>/s calibration discharge, no extrapolation error is present anymore.**

The variation of the spreads for the three Rhine distributaries and the two classification accuracies is summarized in a boxplot (Figure 9). Each red line in Figure 8 that gives the spatial distribution of the spread at the IJssel is represented as a blue box in the lower panel in Figure 9, which also represents the IJssel river. Similar to the spreads in the uncertainty (Figure 6) the extrapolation errors are largest for the IJssel river and smallest for the Bovenrijn-Waal. The same trend of decreasing extrapolation error with the decrease of the extrapolation interval is visible for all three distributaries. The reduction in extrapolation error is small between 3500 and 7000 m<sup>3</sup>/s. This is true for both the classification accuracy of 69% and 95%. However, the extrapolation error is much smaller for a 95% classification accuracy. At the extrapolation interval from 12000 to 16000 m<sup>3</sup>/s, the maximum spread due to a 69% classification accuracy is 12 cm, while at 95% classification accuracy the maximum spread is limited to 4 cm. In general the maximum spread is a factor 2 to 3 higher at 69% classification accuracy.

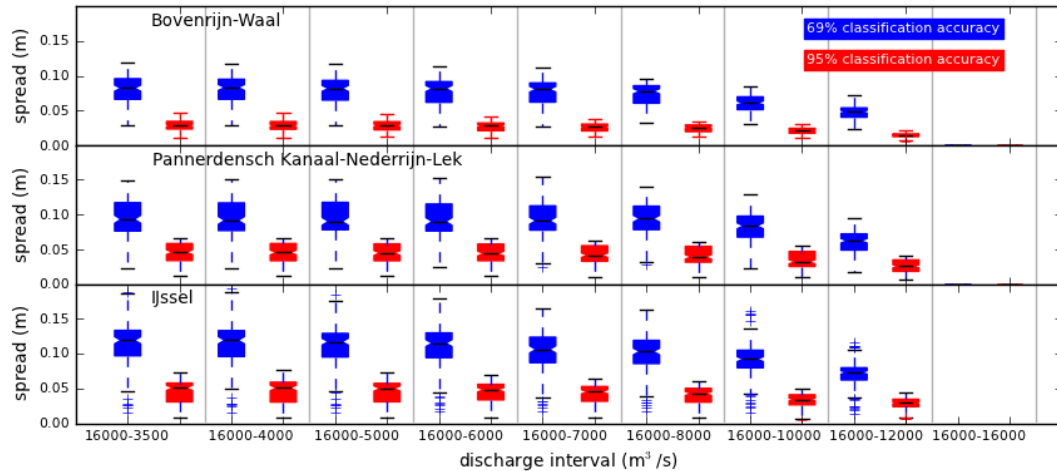


**Figure 9** Extrapolation error in the Rhine distributaries river for different discharges of calibration. The design discharge of 16000 m<sup>3</sup>/s is taken as the reference. The calibration discharge has been varied between 3500 and 12000 m<sup>3</sup>/s. At 16000 m<sup>3</sup>/s calibration discharge, no extrapolation error is present anymore.

To make the results more generic, not only the design discharge was used as the value for extrapolation, but all intervals between the nine stationary discharges (Figure 10,11; table 6). These figures should be read by following the lines from the bottom upwards. The lower point represents the calibration discharge, while the upper part represents the discharge level for extrapolation. For example, the extrapolation error in the Pannerdensch Kanaal, Nederrijn and Lek (Figure 10) is 5 cm when extrapolated from 10000 to 12000 m<sup>3</sup>/s and 13 cm when extrapolated from 10000 to 16000 m<sup>3</sup>/s. Note that these are the maximum spreads per distributary and extrapolation interval. The range will be larger (Figure 8), but the median spread will be lower (Figure 9).

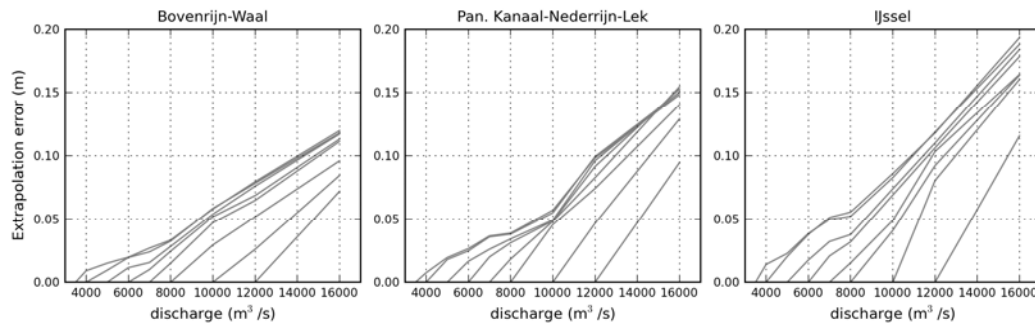


**Figure 10** Extrapolation error between different discharges at 69% classification accuracy. Figure should be read as follows: the extrapolation error in the Pannerdensch Kanaal, Nederrijn and Lek is 5 cm when extrapolated from 10000 to 12000 m<sup>3</sup>/s and 13 cm when extrapolated from 10000 to 16000 m<sup>3</sup>/s.

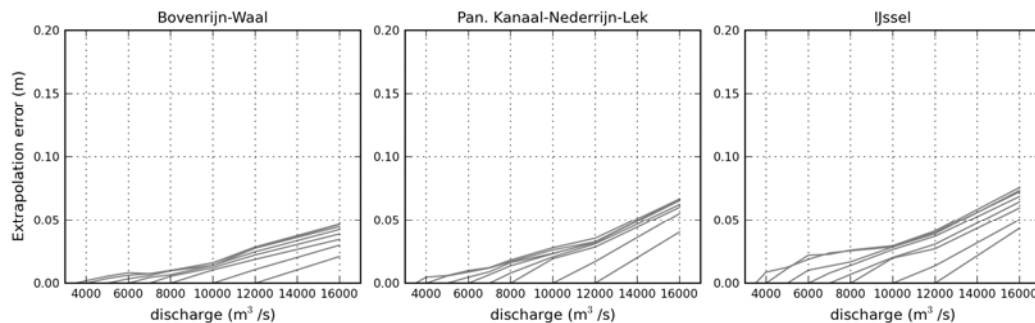


**Figure 11** Extrapolation error in water levels between different discharges at 95% classification accuracy. Increasing the classification accuracy from 69% to 95% reduces the extrapolation error by 60%.

Extrapolation error generally exhibits a linear relationship with the extrapolation interval. The slope of the lines varies between the distributaries and classification accuracy. At 69% classification accuracy, the slope varies between 1 cm/1000 m<sup>3</sup>/s extrapolation interval for the Bovenrijn-Waal to 3 cm/1000m<sup>3</sup>/s for the IJssel river. At 95% classification accuracy the increase in maximum spread is 0.4 cm/1000 m<sup>3</sup>/s extrapolation interval for the Bovenrijn-Waal to 1 cm/1000 m<sup>3</sup>/s for the IJssel river. The highest slopes of the lines are found with the calibration level at 12000 m<sup>3</sup>/s.

The most obvious deviations of the overall linearity are found at lower discharges. For example, the dip in the lines at a 10000 m<sup>3</sup>/s flow rate in the Pannerdensch Kanaal-Nederrijn-Lek (Figure 10) is caused by the small increase in extrapolation error between 6000 and 10000 m<sup>3</sup>/s flow rates. In other words, the maximum spread of the extrapolation from 4000 to 7000 m<sup>3</sup>/s is not much lower than the maximum spread in the extrapolation error at 8000 m<sup>3</sup>/s when calibrated at 4000 m<sup>3</sup>/s. Another striking feature is the crossing of the lines between 12000 and 16000 m<sup>3</sup>/s for the Pannerden-Lek distributary. The lines starting at calibration discharges between 3500 and 7000 m<sup>3</sup>/s overlap, which can be attributed to small changes in extrapolation error, and the use of the maximum spread for this figure. The maximum is more sensitive to outliers than the median spread.

**Table 6 Extrapolation error in water levels between different extrapolation intervals. The upper part of the table gives the spread, the lower part the range. Errors should be determined from lower to higher discharge, e.g. the range in the extrapolation error for the river Waal is 0.14 m when calibrated at 8000 m<sup>3</sup>/s and extrapolated to 12000 m<sup>3</sup>/s. Example printed in bold**

Bovenrijn-Waal		Spread								
69% CA	Q / Q m <sup>3</sup> /s	3500	4000	5000	6000	7000	8000	10000	12000	16000
Range	3500		0.01	0.02	0.02	0.03	0.03	0.06	0.08	0.12
	4000	0.01		0.01	0.02	0.02	0.03	0.06	0.08	0.12
	5000	0.03	0.02		0.01	0.02	0.03	0.05	0.08	0.12
	6000	0.04	0.04	0.03		0.01	0.02	0.05	0.07	0.11
	7000	0.06	0.05	0.05	0.02		0.02	0.05	0.06	0.11
	8000	0.07	0.07	0.06	0.04	0.03		0.03	0.05	0.1
	10000	0.13	0.12	0.11	0.1	0.09	0.07		0.03	0.08
	12000	0.2	0.19	0.18	0.16	0.15	<b>0.14</b>	0.07		0.07
	16000	0.29	0.29	0.28	0.26	0.25	0.23	0.17	0.12	

Pann. Kan.-Nederrijn-Lek		Spread								
69% CA	Q / Q m <sup>3</sup> /s	3500	4000	5000	6000	7000	8000	10000	12000	16000
Range	3500		0.01	0.02	0.03	0.04	0.04	0.06	0.1	0.15
	4000	0.01		0.02	0.02	0.04	0.04	0.06	0.1	0.15
	5000	0.04	0.03		0.02	0.03	0.03	0.05	0.1	0.15
	6000	0.05	0.05	0.03		0.02	0.03	0.05	0.09	0.15
	7000	0.07	0.06	0.05	0.04		0.02	0.05	0.08	0.15
	8000	0.09	0.08	0.07	0.06	0.03		0.05	0.07	0.14
	10000	0.11	0.11	0.1	0.1	0.1	0.09		0.05	0.13
	12000	0.2	0.2	0.2	0.21	0.21	0.2	0.11		0.09
	16000	0.37	0.37	0.36	0.36	0.35	0.35	0.28	0.23	

IJssel		Spread								
69% CA	Q / Q m <sup>3</sup> /s	3500	4000	5000	6000	7000	8000	10000	12000	16000
Range	3500		0.01	0.02	0.04	0.05	0.05	0.08	0.12	0.19
	4000	0.02		0.02	0.04	0.05	0.06	0.09	0.12	0.19
	5000	0.06	0.05		0.02	0.03	0.04	0.07	0.11	0.18
	6000	0.09	0.08	0.04		0.02	0.03	0.07	0.11	0.18
	7000	0.13	0.13	0.08	0.06		0.02	0.05	0.1	0.16
	8000	0.14	0.13	0.11	0.11	0.05		0.04	0.09	0.16
	10000	0.2	0.2	0.19	0.18	0.13	0.09		0.08	0.16
	12000	0.27	0.27	0.25	0.25	0.2	0.17	0.19		0.12
	16000	0.44	0.44	0.43	0.42	0.39	0.37	0.35	0.32	

### 5.2.2 Speed of rise

To understand the relevance of the extrapolation error we need the speed of rise in discharge to understand which of the extrapolation intervals are relevant for the daily forecasts. For a steep increase in discharge little information is available on the actual water levels and a large extrapolation needs to be carried out, while in case a wide peak would occur with a gentle increase in discharge, little extrapolation needs to be carried out with respect to the existing water levels. Therefore all flood peaks between Januari 1901 and August 2007 with peak of more than 5000 m<sup>3</sup>/s and a duration of more than three days are shown in Figure 14. The number of flood peaks amounted to 111 (left panel figure 14). The right panel gives the histogram of the increase in discharge over a one to four day periods. The maximum increase in discharge has been 2115, 3765, 5040, and 6265 m<sup>3</sup>/s over the one to four day period, respectively.

If we assume that the model is calibrated perfectly at 8000 m<sup>3</sup>/s, and that the discharge at a specific moment is also 8000 m<sup>3</sup>/s than the extrapolation error can be computed for one to four day periods. Based on a 69% classification accuracy, an increase of 2115 m<sup>3</sup>/s would give an extrapolation error of 3 cm for the Waal and of 4.5 cm for the IJssel (Figure 12). The maximum increase over 4 days, 6265 m<sup>3</sup>/s, would give an extrapolation error of 7.5 and 12.5 cm for Waal and IJssel, respectively (Figure 12).

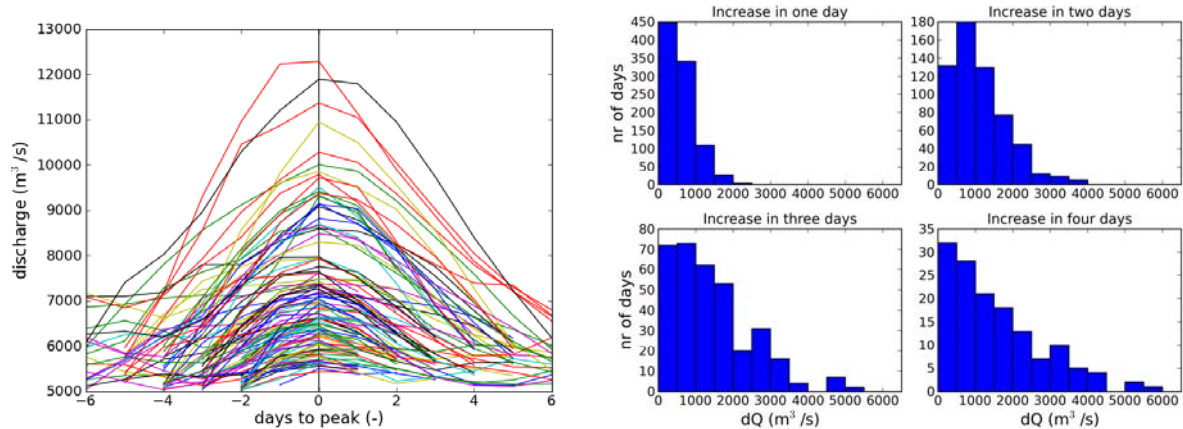


**Figure 12 Flood peaks between Januari 1901 and August 2007 with a peak discharge of more than 5000 m<sup>3</sup>/s and a duration of more than 3 days (left panel), and the speed of increase in discharge (dQ) over a one to four day period (right panel).**

### 5.2.3 Discharge

Depending on the spatial distribution of the floodplain roughness, a distributary will convey more, or less water. Similar to the extrapolation error in the water levels, the extrapolation error in the discharge of the distributaries is affected by the discharge used for calibration (Fig. 13; Table 7). The higher the discharge of the event used for calibration, the lower the extrapolation error in the discharge distribution, and the lower the extrapolation interval, the lower the error.

Calibration may reduce the error, but not remove it completely. At a 69% CA the spread in the Waal design discharge of 16000 m<sup>3</sup>/s is 76 m<sup>3</sup>/s after calibration at 12000 m<sup>3</sup>/s (Fig. 15 top left; Table 7). At 95% CA, the spread in discharge due to extrapolation is reduced to 30 m<sup>3</sup>/s. Increasing the classification accuracy from 69% to 95% reduces the extrapolation error by approximately 60%. The tabular data for the Pannerdensch Kanaal, Nederrijn-Lek and the IJssel river are presented in Appendix 5. Errors in discharge for the Waal, Pannerdensch Kanaal and Nederrijn-Lek show are comparable. The IJssel shows slightly lower extrapolation errors in discharge. The need for high discharge flood events also becomes apparent with respect to the uncertainty reduction in discharge for all distributaries. The calibration events with a discharge between 3500 and 10000 m<sup>3</sup>/s all cluster together with respect to the spread in discharge at 16000 m<sup>3</sup>/s. Only the 12000 m<sup>3</sup>/s event reduces the error significantly. This pattern is contrary to what we observed for extrapolation errors in water levels.

All distributaries show a reduction in the error compared to the uncertainty at the design discharge without calibration (Table 5). For the Waal, the spread and range in discharge without calibration are 89, and 340 m<sup>3</sup>/s, respectively. After calibration at 12000 m<sup>3</sup>/s, the spread and range are reduced to 76 and 191 m<sup>3</sup>/s (Table 7), a 15% reduction in spread and 44% in range.

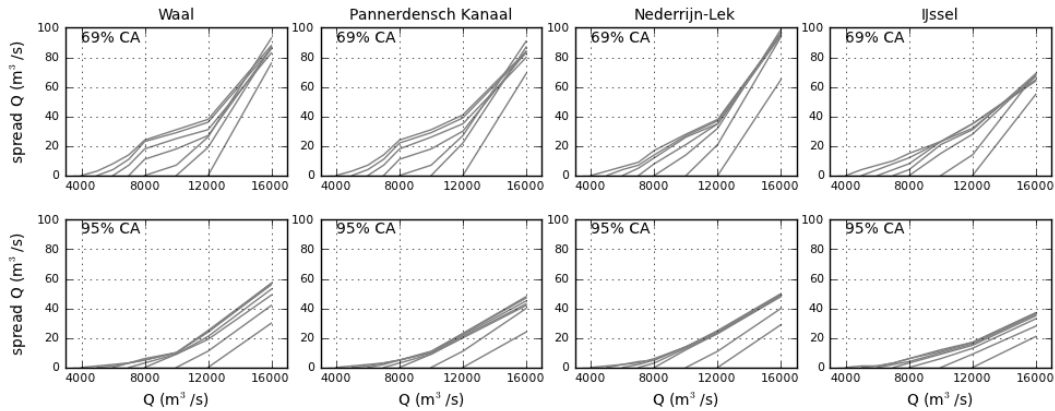


**Figure 13** Extrapolation error in discharge for each of the four river sections: Waal, Pannerdensch Kanaal, Nederrijn-Lek, and IJssel (Figure 3). The top row shows the spread of the extrapolation error due to a 69% classification error. The bottom row shows the same for a 95% classification accuracy.

Figure should be read as by following the lines from the bottom upwards, e.g.: the extrapolation error in the Pannerdensch Kanaal, Nederrijn and Lek is 76 m<sup>3</sup>/s when extrapolated from 12000 to 16000 m<sup>3</sup>/s at 69% CA, and 30 m<sup>3</sup>/s when extrapolated from 12000 to 16000 m<sup>3</sup>/s at 95% CA.

Increasing the classification accuracy from 69% to 95% reduces the extrapolation error by approximately 60%.

**Table 7 Tabular data of the left panels in Fig. 13: Extrapolation error of discharges for the Waal. Spreads discharge are plotted above the diagonal, ranges in discharge below. Extrapolation interval should be read from low to high discharge.**

Waal 69% CA		Spread (m <sup>3</sup> /s)								
Q \ Q		3500	4000	5000	6000	7000	8000	10000	12000	16000
Range (m <sup>3</sup> /s)	3500		1	4	8	15	25	32	40	89
	4000	3		3	8	14	24	31	38	88
	5000	6	5		4	11	23	29	36	86
	6000	12	10	7		7	18	25	31	83
	7000	20	20	16	12		11	18	27	86
	8000	30	29	28	26	15		7	26	93
	10000	78	77	74	70	60	55		19	87
	12000	155	155	151	146	138	127	78		76
	16000	338	337	334	330	319	309	263	191	

Waal 95% CA		Spread (m <sup>3</sup> /s)								
Q \ Q		3500	4000	5000	6000	7000	8000	10000	12000	16000
Range (m <sup>3</sup> /s)	3500		1	2	3	3	5	10	25	58
	4000	2		1	2	3	5	10	24	57
	5000	4	2		1	3	6	10	25	57
	6000	6	5	3		3	5	10	24	56
	7000	11	11	9	6		3	9	21	53
	8000	19	18	16	13	8		9	19	49
	10000	25	24	22	20	15	13		11	42
	12000	38	38	37	37	35	33	23		30
	16000	92	92	91	91	89	87	74	56	

The reduction in the uncertainty in water distribution over the bifurcation points due to calibration is less than difference in spreads for individual discharges. For example, the spread for the Waal is 89 and 40 m<sup>3</sup>/s at a discharge of 16000, and 12000 m<sup>3</sup>/s at Lobith, respectively (Table 5), a difference of 49 m<sup>3</sup>/s. The spread in the Waal discharge is 76 m<sup>3</sup>/s when calibrated at 12000 m<sup>3</sup>/s and extrapolated to 16000 m<sup>3</sup>/s, which gives a reduction of 13 m<sup>3</sup>/s with the spread at 16000 m<sup>3</sup>/s without calibration. The small reduction in spread resulted from difference the ranking in the individual runs per discharge level. The roughness realization that gives the highest discharge at 12000 m<sup>3</sup>/s is not necessarily the same that gives the highest discharge for that distributary at 16000 m<sup>3</sup>/s. This is illustrated in Fig. 16 showing the scatter plots of the Waal discharges between four different flow rates at the upstream boundary. The reason for the difference in ranking is that different floodplain areas exert a dominant influence on the discharge distribution depending on flow rate. Since the spread after calibration is computed on the set of differences based on individual roughness realizations, the reduction in the uncertainty due to calibration is less the uncertainty at the two different levels.

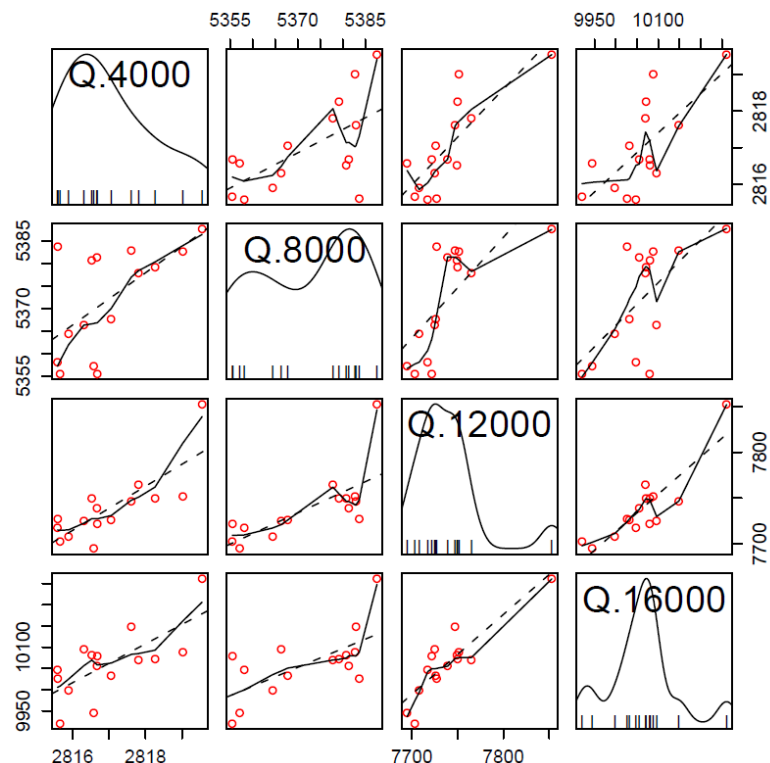


**Figure 14 Scatterplot matrix of discharges for the Waal distributary at four flow rates at the upstream boundary condition ( $Q = 4000, 8000, 12000, 16000 \text{ m}^3/\text{s}$ ).**

### 5.3 CURRENT PREDICTION ACCURACY

To fill the gap in the overview of the prediction accuracy during flood events, WE analysed the forecasts since the availability of the four day lead times. These were available since April 2001. Events were selected with a peak water level of more than 12 m +NAP and a duration of more than three days. In total 20 events were selected (Figure 17). The water level predictions for the Lobith gauging station showed large differences in accuracy between the different flood events. From the perspective of flood management, the prediction accuracy of the peak of the flood event is particularly relevant. The peak of the flood events were often overpredicted, such as the Januari events in 2002, 2004, and 2011. The overprediction was not systematic as the flood events of March 2002, Januari 2003, or April 2006 showed.

Table 6 list the 20 events chronologically. The forecasts with a one to four day lead time showed an average mean absolute error (MAE) of 6, 14, 28, and 53 cm, respectively. This shows that the desired accuracy of 10, 15, 20, and 40 cm prediction accuracy for the 1-4 day forecast is not always reached. One day forecasts are within the desired accuracy 81 % of the time, while the 3 and 4 day forecasts proved to be accurate only 49, and 54 % of the time, respectively. The mean absolute error of the prediction does not show a clear trend over

time (Fig. 18). A regression analysis even showed an increase in MAE with time (results not shown), although it was a weak relation. However, the increase was strongly influenced by large MAE of the flood event of January 2011. Without this event no increase in MAE was present in the data.

The to relate the extrapolation error due to classification errors in floodplain vegetation to the forecast error, we can look at the extrapolation error for the design discharge, when calibrated at 12000 m<sup>3</sup>/s and compare it to the 4 day prediction error. The average four day prediction error is 53 cm, while the extrapolation error is 12 cm. Under these conditions, the vegetation is a substantial error source for the accurate prediction of the water level predictions. For minor flood peaks, up to 8000 m<sup>3</sup>/s, the vegetation is not an important source of uncertainty at these discharge levels.

**Table 8 Overview of one to four day prediction accuracy of flood events since 2001.**

Peak <sup>a</sup>	max h (cm +NAP) <sup>b</sup>	MAE day-1	MAE day-2	MAE day-3	MAE day-4	Length Peak (days)	Nr days beyond 10 cm desired accuracy	Nr days beyond 15 cm desired accuracy	Nr days beyond 20 cm desired accuracy	Nr days beyond 40 cm desired accuracy
2001.April.20	1279	3	8	16	27	11	0	1	3	2
2001.May.02	1230	3	5	9	17	7	0	0	1	1
2001.December.05	1261	7	19	25	51	4	0	2	3	3
2002.January.31	1378	8	22	39	72	8	1	4	5	6
2002.February.17	1374	5	16	36	64	7	2	3	4	4
2002.March.02	1505	6	17	31	40	16	3	6	10	7
2002.March.25	1448	6	8	22	47	8	1	1	3	3
2002.November.15	1412	10	12	16	23	21	9	4	6	4
2003.January.07	1568	7	15	26	54	17	4	6	7	10
2004.January.19	1426	8	19	30	57	10	2	5	7	5
2005.February.17	1337	8	18	44	82	5	2	3	3	2
2006.March.14	1349	9	9	56	106	5	3	1	5	5
2006.April.04	1352	5	13	12	29	10	0	3	1	4
2007.February.17	1255	5	25	36	81	4	0	2	1	3
2007.March.06	1376	4	9	37	65	8	0	2	8	5
2007.December.13	1325	3	12	20	46	10	0	3	5	5
2009.March.15	1225	5	11	15	20	4	0	1	1	1
2010.March.03	1322	7	13	21	42	6	1	2	3	1
2010.December.14	1354	6	10	20	52	6	2	1	4	4
2011.January.17	1515	9	29	54	77	16	5	8	13	10
<b>Average</b>		<b>6</b>	<b>14</b>	<b>28</b>	<b>53</b>		<b>81%</b>	<b>68%</b>	<b>49%</b>	<b>54%</b>

<sup>a</sup> Date of the peak of the flood event, links to the date in Figure 12.

<sup>b</sup> Maximum recorded water level at Lobith gauging station during the event.

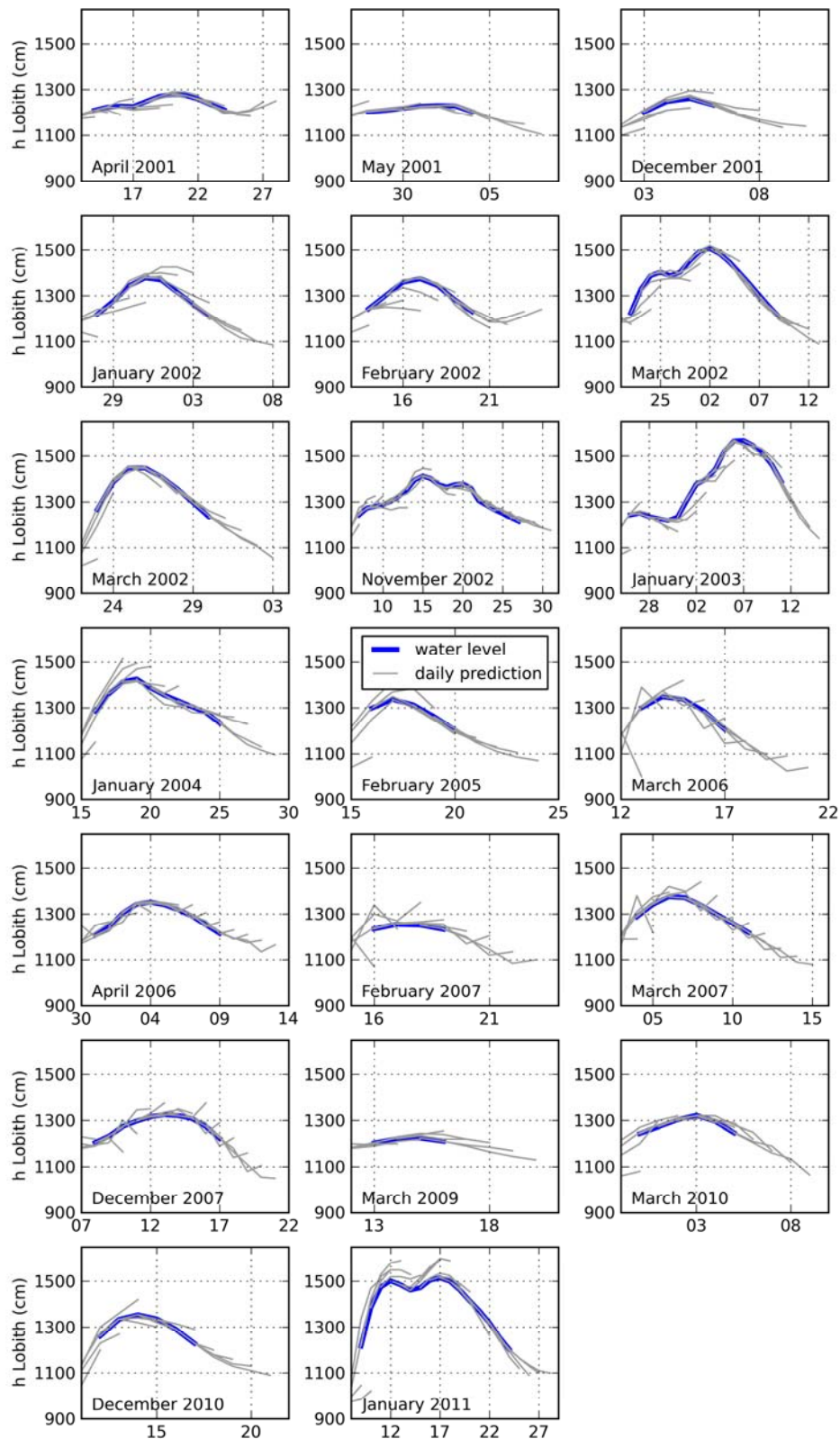


**Figure 15 Flood events (water level Lobith > 12m, duration > three days) and daily four-day forecasts for the Lobith gauging station between 2001 and 2011.**

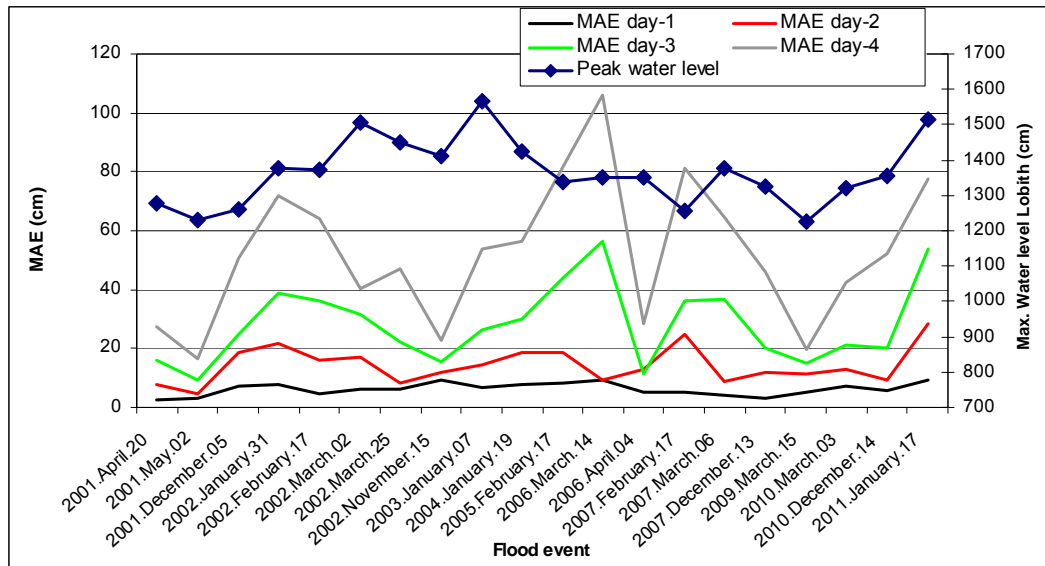


Figure 16 Prediction error of 1-4 day lead times for all flood peaks higher than 12 m at Lobith over the period April 2001 till Januari 2011.

## 6 DISCUSSION

Hydrodynamic models are routinely used for water level predictions beyond the flood events used for calibration. In this extrapolation there is no means of correcting for errors in the model setup resulting flood roughness parameterization. In this study, the extrapolation error has been quantified for the first time in a 2D hydrodynamic model with respect to water levels and discharge distribution. We used an example of the Rhine distributaries in The Netherlands.

The map purity table underlies the assignment of new ecotopes to all the polygons in the 30 realizations. However the table has been altered twice. Once to include the ecotopes that were not identified in the field campaign (Knotters et al., 2008) and to standardize rows and columns of the map purity table. These steps have been listed in Straatsma and Alkema (2009). The second time the map purity table was changed was to simulate a 95% classification accuracy at ecotope group level (this study). After that the ecotopes of the revised version of the second ecotope mapping cycle had to be recoded to the unrevised version. These steps introduced errors on top of the errors in the validation due to support and identifiability of ecotopes in the field. We believe the outcome is plausible and realistic, but still a number arbitrary decisions needed to be made. That would have been unnecessary if the ecotope map was properly validated, and iterates the point that a map needs to be accompanied with an undisputed validation. In anticipation of a future undisputed validation, we showed that a 95%CA resulted in a 60% reduction of the spread in water levels.

The uncertainty in water levels at the design discharge, reported as the spread are smaller in this study compared to the results of last year (Straatsma and Huthoff, 2010; Straatsma and Huthoff, 2011). In this study, the spreads at a design discharge of 16000 m<sup>3</sup>/s (table 5) are 30% lower in this study compared to the previous study. The reasons might be twofold. Firstly, the polygon size increased. In 2010, we used the area-u and area-v files for realization of new roughness files, without using Baseline. The area files are based on the aggregated ecotopes into the 16 roughness classes. Due to the aggregation, the mean polygon size increased from 20700 m<sup>2</sup> ( $\sigma=463200$  m<sup>2</sup>) to 50500 m<sup>2</sup> ( $\sigma=725700$  m<sup>2</sup>). As we only altered the roughness code of the aggregated ecotopes, we imposed a spatial correlation in the roughness map that might not be present in the original ecotope map. The effect of spatial correlation was studied as the scale error by (Straatsma and Huthoff, 2011), who showed that smaller polygons lead to a smaller error, as smaller areas will change from one ecotope to another. The factor reduction in mean polygon size by 60% would therefore be accountable for a large part of the reduction in the uncertainty in the water levels. Secondly, the number of realizations of the ecotope map could affect the uncertainty. The 15 realizations that we used gave fairly stable results, but small changes in uncertainty could be due to specific realizations of the ecotope map. Were more extreme roughness values chosen in the random sampling, the uncertainty could be slightly larger, in the order of 1 or 2 cm increase in spread. The xtrapolation error could be reduced to only 30% of the currently estimated values, if the correction factor as proposed in the appendix is used. In that case a spread of 4 cm for the IJssel would the uncertainty from floodplain roughness parameterization.

A trade-off exists between the different flood events that can be used for model calibration. In The Netherlands, a 12000 m<sup>3</sup>/s flood event is used for calibration (Jan. 1995), while the design discharge is 16000 m<sup>3</sup>/s. In January 2003, a 10000 m<sup>3</sup>/s flood event occurred. Both events could be used for calibration of the model, leading to a trade-off between representing the current layout of the floodplains and the extrapolation error. Since 1995 a large number of landscaping measures have been implemented that affected both the morphology and the roughness of the floodplain area. Therefore, the 2003 event represents the current distribution of roughness and bathymetry better than the 1995 event. The 1995 event has a smaller extrapolation error, because the extrapolation interval is 4000 m<sup>3</sup>/s instead of 6000 m<sup>3</sup>/s for the 2003 event. The extrapolation error is reduced by 1, 4, and 4 cm for Bovenrijn-Waal, Pannerdensch Kanaal-Nederrijn-Lek, and IJssel respectively when the 1995 event is used instead of the 2003 event. What the effects are of using the 1995 spatial model input and using those results for 2011 is unknown to the authors and it can not be derived from the current model output.

In this study, we assume a perfectly calibrated model and only look at the extrapolation error. In reality, the model will not be perfectly calibrated and there are a number of other error sources that may contribute to the total error in the predicted water levels at design water levels. Other error sources could be quantified in the same way to come to a complete overview of the modeling error. Warmink et al. (submitted) combined several error sources in roughness parameterization of the main channel and the floodplain for the river Waal. The total uncertainty in the water levels showed a 95% confidence interval of 61 cm based on the combined effect of main channel roughness, floodplain classification accuracy, within class variation of vegetation structural

characteristics, and choice of roughness model. These results do not take calibration into account. Assuming the calibration at  $12000 \text{ m}^3/\text{s}$  also leads to a reduction in uncertainty of 50 % for all these error sources, the absolute 95 % confidence interval in the water levels for the river Waal would be around 30 cm. This is four times higher than the 7 cm absolute 68% confidence interval found in this study. Based on a normal distribution, the 95% confidence interval is twice the 68% confidence interval, which would give a 14 cm absolute uncertainty at the 95% confidence interval for the Waal due to floodplain roughness uncertainty. This might be half of the total uncertainty due to the uncertainty from all roughness errors.

In operational flood forecasting, the aim is to provide a 10, 15, 20, and 40 cm accuracy for the one to four day forecasts, respectively. We showed that the uncertainty in water levels beyond the calibration event (7 to 12 cm) may be an important source of error at high discharges. While at flood events below the calibration discharge this error source might be less relevant, it is less likely that a flood peak with a  $16000 \text{ m}^3/\text{s}$  flow rate will be forecasted within the required accuracy. The only way to improve these forecasts is to make sure that the classification accuracy of the ecotope map is determined accurately and improved if needed.



## 7 CONCLUSIONS AND RECOMMENDATIONS.

In this study, we simulated two sets of 15 landcover maps using a Monte Carlo analysis based on the ecotope map of the Rhine distributaries and the map purity table. One set represented a classification accuracy of 69% at ecotope group level, the other a 95% classification accuracy. Based on the differences in water level between the calibration flood event and the flood event with a higher discharge, we were able to determine the extrapolation error for different extrapolation intervals. Based on this new methodology to determine the extrapolation error, we conclude that:

- > Calibration at 12000 m<sup>3</sup>/s reduces the uncertainty at 16000 m<sup>3</sup>/s discharge by 50%, independent on the classification accuracy of the ecotope map.
- > The extrapolation error, quantified as the maximum spread per distributary shows a linear relationship with the extrapolation interval in discharge.
- > The slope of this linear line differs between the distributaries. At 69% classification accuracy, the slope varies between 1 cm/1000 m<sup>3</sup>/s extrapolation interval for the Bovenrijn-Waal to 3 cm/1000m<sup>3</sup>/s for the IJssel river. At 95% classification accuracy the increase in maximum spread is 0.4 cm/1000 m<sup>3</sup>/s extrapolation interval for the Bovenrijn-Waal to 1 cm/1000 m<sup>3</sup>/s for the IJssel river. The highest slopes of the lines are found with the calibration level at 12000 m<sup>3</sup>/s.
- > The extrapolation error with a calibration event of 12000 m<sup>3</sup>/s and a design discharge of 16000 m<sup>3</sup>/s is 7, 9, 12 cm for the Bovenrijn-Waal, Pannerdensch Kanaal-Nederrijn-Lek, and IJssel river, respectively. This is based on a 69% CA. At 95% CA, the errors are 2, 4, and 4 cm respectively.
- > For an increased design discharge of 18000, or 20000 m<sup>3</sup>/s the extrapolation error might increase to 24 cm for the IJssel, and 14 cm for the Bovenrijn-Waal.
- > The range in uncertainty is more than three times higher than the spread.
- > The uncertainty in discharge distribution is less affected by calibration than the uncertainty in water levels. The uncertainty reduced by 15% when calibrated at 12000 m<sup>3</sup>/s.

Based on an the analysis of all flood peaks between 1901 and 2007 we determined the speed of rise during the flood events. The maximum increase in discharge has been 2115, 3765, 5040, and 6265 m<sup>3</sup>/s over the one to four day period, respectively. This can be converted to uncertainty in water levels, e.g. assuming a calibration at 10000 m<sup>3</sup>/s, this would lead to 5-13 cm uncertainty for the Nederrijn-Lek. The xtrapolation error could be reduced to only 30% of the currently estimated values, if the correction factor as proposed in the appendix is used. In that case a spread of 4 cm for the IJssel would the uncertainty from floodplain roughness parameterization.

## REFERENCES

- Baptist, M.J., Babovich, V., Rodríguez Uthurburu, J., Keijzer, M., Uittenbogaard, R.E., Mynett, A., Verwey, A., 2007. On inducing equations for vegetation resistance. *Journal of hydraulic research* 45, 435-450.
- Baptist, M.J., Penning, W.E., Duel, H., Smits, A.J.M., Geerling, G.W., Van der Lee, G.E.M., Van Alphen, J.S.L., 2004. Assessment of the effects of cyclic floodplain rejuvenation on flood levels and biodiversity along the Rhine River. *River Research and Applications* 20, 285-297.
- Geerling, G.W., Labrador-Garcia, M., Clevers, J., Ragas, A., Smits, A.J.M., 2007. Classification of floodplain vegetation by data-fusion of Spectral (CASI) and LiDAR data. *International Journal of Remote Sensing* 28, 4263 – 4284.
- Hartman, M.R., Van den Braak, W.E.W., 2007. Baseline manual, baseline 4.03. RIZA, Arnhem, report nr. RIZA-werkdocument 2004-170X, pp. 128.
- Huthoff, F., Augustijn, D., 2004. Sensitivity analysis of floodplain roughness in 1D flow. In: Liong, S.Y., Phoon, S.I., Babovich, V. (Eds.), 6th International conference on hydroinformatics, Singapore, Malaysia, pp. 301-308.
- Huthoff, F., Augustijn, D.C.M., Hulscher, S.J.M.H., 2007. Analytical solution of the depth-averaged flow velocity in case of submerged rigid cylindrical vegetation. *Water Resources Research* 43, (W06413).
- Jansen, B.J.M., Backx, J.J.G.M., 1998. Ecotope mapping Rhine Branches-east 1997 (in Dutch). RIZA, Lelystad, report nr. 98.054, pp. 41.
- Jesse, P., 2004. Hydraulic resistance in (nature) development (in Dutch). RIZA, Arnhem, report nr. RIZA werkdocument, 2003.124X, pp. 65.
- Klopstra, D., Barneveld, H., Van Noortwijk, J.M., Van Velzen, E.H., 1997. Analytical model for hydraulic roughness of submerged vegetation. 27th international IAHR conference San Francisco, pp. 775-780.
- Knotters, M., Brus, D.J., conditionally accepted. Sampling for validation of ecotope maps of floodplains in the Netherlands. *Journal of Environmental Management*.
- Knotters, M., Brus, D.J., Heidema, A.H., 2008. Validatie van de ecotopenkaarten van de rijkswateren. Alterra, Wageningen, report nr. Alterra-rapport 1656, pp. 47.
- Kouwen, N., 2000. Friction factors for coniferous trees along rivers. *Journal of hydraulic engineering* 126, 732-740.
- Kouwen, N., Li, R.M., 1980. Biomechanics of vegetated channel linings. *Journal of Hydraulics Divisions* 106, 1085-1103.
- Lindström, G., Johansson, B., Persson, M., Gardelin, M., Bergström, S., 1997. Development and test of the distributed HBV-96 hydrological model. *Journal of Hydrology* 201, 272-288.
- Petryk, S., Bosmajian, G., 1975. Analysis of flow through vegetation. *Journal of Hydraulics Divisions* 101, 871-884.
- Reggiani, P., Renner, M., Weerts, A.H., Van Gelder, P.A.H.J.M., 2009. Uncertainty assessment via Bayesian revision of ensemble streamflow predictions in the operational river Rhine forecasting system. *Water Resources Research* 45.
- Reggiani, P., Weerts, A.H., 2008. A Bayesian approach to decision-making under uncertainty: An application to real-time forecasting in the river Rhine. *Journal of Hydrology* 356, 56-69.
- RWS, 2007. Users guide WAQUA: Technical Report SIMONA 92-10. <http://www.waqua.nl/systeem/documentatie/usedoc/slib3d/ug-slib3d.pdf>, date accessed 13-02-2008.
- Schumann, G., Di Baldassarre, G., Bates, P.D., 2009. The utility of spaceborne radar to render flood inundation maps based on multialgorithm ensembles. *IEEE transactions on geoscience and remote sensing* 47, 2801-2807
- Sprokkedreef, E., 2001. FloRIJN 2000: Verlenging van de zichttijd van hoogwatervoorspellingen voor de Rijn in Nederland tot drie dagen. RIZA, Lelystad, report nr. RIZA rapport 2001.060, pp. 68.
- Stolker, C., Van Velzen, E.H., Klaassen, G.J., 1999. Nauwkeurigheidanalyse stromingsweerstand vegetatie (in Dutch). Delft Hydraulics, RIZA, Delft, Arnhem, report nr. 99.192x, pp. 21.
- Straatsma, M., Huthoff, F., 2011. Uncertainty in 2D hydrodynamic models from errors in roughness parameterization based on aerial images. *Physics and Chemistry of the Earth, Parts A/B/C* 36, 324-334.
- Straatsma, M.W., Alkema, D., 2009. Error propagation in hydrodynamics of lowland rivers due to uncertainty in vegetation roughness parameterization FloodControl2015, report nr. 2009-06-05, pp. 44.
- Straatsma, M.W., Baptist, M.J., 2008. Floodplain roughness parameterization using airborne laser scanning and spectral remote sensing. *Remote Sensing of Environment* 112, 1062-1080.
- Straatsma, M.W., Huthoff, F., 2010. Relation between accuracy of floodplain roughness parameterization and uncertainty in 2D hydrodynamic models. Faculty of ITC, University of Twente, Enschede, report nr. pp. 49.

- Sumihar, J., Verlaan, M., Weerts, A., Schroevers, R., 2009. Uncertainty analysis on waterlevels and discharges produced by data model integrated systems. Deltares, Delft, report nr. 1200087-000-ZWS-0008, pp. 43.
- Van der Molen, D.T., Geilen, N., Backx, J.J.G.M., Jansen, B.J.M., Wolfert, H.P., 2003. Water Ecotope Classification for integrated water management in the Netherlands. European Water Management Online. [http://www.ewaonline.de/journal/2003\\_03.pdf](http://www.ewaonline.de/journal/2003_03.pdf), date accessed
- Van der Sande, C.J., De Jong, S.M., De Roo, A.P.J., 2003. A segmentation and classification approach of IKONOS-2 imagery for land cover mapping to assist flood risk and flood damage assessment. International Journal of Applied Earth Observation and Geoinformation 4, 217-229.
- Van Rijn, L.C., 1994. Principles of fluid flow and surface waves in rivers, estuaries, seas and oceans. Aqua publications, Amsterdam.
- Van Stokkom, H.T.C., Smits, A.J.M., Leuven, R.S.E.W., 2005. Flood defense in the Netherlands a new era, a new approach. Water International 30, 76-87.
- Van Velzen, E.H., Jesse, P., Cornelissen, P., Coops, H., 2003. Stromingsweerstand vegetatie in uiterwaarden (in Dutch). RIZA, Arnhem, report nr. 2003.028, pp. 131.
- Warmink, J.J., Huthoff, F., Straatsma, M.W., Booij, M.J., Van der Klis, H., Hulscher, S.J.M.H., submitted. Combining uncertainty in channel and floodplain roughness to assess the uncertainty in design water levels for a lowland alluvial river. Water Resources Research.
- Weerts, A., 2008. Hindcast of water levels for the Rhine branches and the Meuse for 2006 & 2007. Deltares, Delft, report nr. Q4234, pp. 16.
- Weerts, A., El Serafy, G.Y., Hummel, S., Dhondia, J., Gerritsen, H., 2010. Application of generic data assimilation tools (DATools) for flood forecasting purposes. Computers and Geosciences 36, 453-463.



# APPENDIX 1 : ADJUSTED ERROR MATRIX

Dark yellow rows and columns have been adjusted, compared to Knotters et al. (2008). See Straatsma and Alkema (2009) for background information.

ECOCODE	H-REST	HA-1	HA-2	HB-1	HB-2	HB-3	HG-1	HG-1-2	HG-2	HM-1	HR-1	I.1	II.2	III.2-3
H-REST	0.162	0	0.486	0	0.353	0	0	0	0	0	0	0	0	0
HA-1	0	0	0	0	0	0	0	0	0.071	0	0	0	0	0
HA-2	0	0	0.842	0	0	0.018	0	0	0.018	0	0	0	0	0
HB-1	0	0	0.298	0.318	0	0.06	0	0	0	0	0	0	0	0
HB-2	0	0	0.092	0.105	0.214	0.02	0.054	0	0	0	0.054	0	0	0
HB-3	0	0	0.138	0	0.18	0.222	0	0	0	0	0	0	0	0
HG-1	0	0	0	0	0	0	0.15	0	0.172	0	0	0	0	0
HG-1-2	0	0	0	0	0	0	0	0	0.496	0	0	0	0	0
HG-2	0	0.009	0	0	0	0.052	0	0.078	0.193	0	0	0	0	0
HM-1	0	0	0	0	0	0	0	0	0	0	0	0	0	0
HR-1	0	0	0	0	0.079	0	0.093	0	0.079	0	0.289	0	0	0
I.1	0	0	0	0	0	0	0	0	0	0	0	1	0	0
II.2	0	0	0	0	0	0	0	0	0	0	0	0	0.858	0
III.2-3	0	0	0.2	0	0	0	0	0	0	0	0	0	0	0
IV.8-9	0	0	0	0	0	0	0	0	0	0	0	0	0	0
IX.a	0	0	0	0	0	0	0	0	0	0	0	0	0	0
O-U-REST	0.2	0	0	0	0	0	0	0	0	0	0	0	0	0
O-UA-1	0	0	0	0	0	0	0.05	0.05	0	0	0	0	0	0
O-UA-2	0	0	0	0	0	0	0	0	0	0	0	0	0	0
O-UB-1	0	0	0	0	0	0	0	0	0	0	0	0	0	0
O-UB-2	0	0	0	0.098	0	0	0	0	0	0	0	0	0	0
O-UB-3	0	0	0	0	0	0.15	0	0	0	0	0	0	0	0
O-UG-1	0	0	0	0	0	0	0	0	0	0	0	0	0	0
O-UG-1-2	0	0	0	0	0	0	0	0	0	0	0	0	0	0
O-UG-2	0	0	0	0	0	0	0	0	0	0	0	0	0	0
O-UK-1	0	0	0	0	0	0	0	0.1	0	0	0	0	0	0
O-UR-1	0	0	0	0	0	0	0	0	0	0	0	0	0	0
OK-1	0	0	0	0	0	0	0	0	0	0	0	0	0	0
R	0	0	0	0	0	0	0	0	0	0	0	0	0.35	0
REST	0	0	0	0	0	0	0	0	0	0	0	0	0.685	0
RnM	0	0	0	0	0	0	0	0	0	0	0	0	0	0
RvD	0	0	0	0	0	0	0	0	0	0	0	0	0	0
RvM	0	0	0	0	0	0	0	0	0	0	0	0	0	0
RvO	0	0	0	0	0	0	0	0	0	0	0	0	0	0
RwD	0	0	0	0	0	0	0	0	0	0	0	0	0	0
RwM	0	0	0	0	0	0	0	0	0	0	0	0	0	0
RwO	0	0	0	0	0	0	0	0	0	0	0	0	0	0
RzD	0	0	0	0	0	0	0	0	0	0	0	0	0	0
RzM	0	0	0	0	0	0	0	0	0	0	0	0	0	0
RzO	0	0	0	0	0	0	0	0	0	0	0	0	0	0
U-REST	0	0	1	0	0	0	0	0	0	0	0	0	0	0
UA-1	0	0.108	0	0	0	0	0	0	0	0	0	0	0	0
UA-2	0	0	0.486	0	0	0	0	0	0	0	0	0	0	0
UB-1	0	0	0	0	0.068	0	0	0	0	0	0	0	0	0
UB-2	0	0	0	0	0.245	0.105	0	0	0	0	0.105	0	0	0
UB-3	0	0	0	0	0	0.119	0	0	0	0	0	0	0	0
UG-1	0	0	0	0	0	0	0.042	0	0.042	0	0	0	0	0
UG-1-2	0	0	0	0	0	0.037	0	0	0.123	0	0.085	0	0	0
UG-2	0	0	0	0	0	0	0	0	0	0	0	0	0	0
UM-1	0	0	0	0	0	0	0	0	0	0	0	0	0	0
UR-1	0.094	0	0	0	0	0	0	0	0	0	0	0	0	0
V.1-2	0	0	0	0	0	0	0	0	0	0	0	0	0	0
VI.2-3	0	0	0	0	0	0	0	0	0.06	0	0	0	0	0
VI.4	0.087	0	0	0	0	0	0	0	0	0	0	0	0	0
VI.7	0	0	0	0	0	0	0	0	0	0	0	0	0	0
VI.8	0	0	0	0	0	0.181	0	0	0	0	0	0	0	0
VII.1	0	0	0	0	0	0	0	0	0	0	0	0	0	0
VII.1-3	0	0	0	0	0	0	0	0	0.137	0	0	0	0	0
VII.3	0	0	0	0	0	0	0	0	0	0	0	0	0.321	0

ECOCODE	IV.8-9	IX.a	O-U-REST	O-UA-1	O-UA-2	O-UB-1	O-UB-2	O-UG-1	O-UG-1-2	O-UG-2	O-UK-1	O-UR-1	OK-1	R
H-REST	0	0	0	0	0	0	0	0	0	0	0	0	0	0
HA-1	0	0	0	0.167	0	0	0	0	0	0	0	0	0	0
HA-2	0	0	0	0	0.055	0	0.018	0	0	0	0	0	0	0
HB-1	0	0	0	0	0	0	0.117	0	0	0	0	0	0	0
HB-2	0	0	0	0	0	0	0.079	0	0	0	0	0	0	0
HB-3	0	0	0	0	0	0	0	0	0	0	0	0	0	0
HG-1	0	0	0	0.13	0.075	0	0	0.113	0	0.086	0	0	0	0
HG-1-2	0.257	0	0	0	0	0	0	0	0	0	0	0	0	0
HG-2	0	0	0	0	0	0	0.026	0.074	0	0.136	0	0	0	0
HM-1	0	0	0	0	0	0	0	0	0	0	0	0	0	0
HR-1	0.101	0	0	0	0	0	0	0	0	0	0	0.035	0	0
I.1	0	0	0	0	0	0	0	0	0	0	0	0	0	0
II.2	0	0	0	0	0	0	0	0	0	0	0	0	0	0
III.2-3	0	0	0	0	0.599	0	0.2	0	0	0	0	0	0	0
IV.8-9	0.834	0	0	0	0	0	0	0	0	0	0	0	0	0
IX.a	0	0	0	0	0	0	0	0	0	0	0	0	0	0
O-U-REST	0	0	0.3	0.1	0	0	0	0	0	0	0	0	0.1	0
O-UA-1	0	0	0.1	0.6	0	0	0	0.05	0.05	0.1	0	0	0	0
O-UA-2	0	0	0	0	0	0	0	0	0	0	0	0	0	0
O-UB-1	0	0	0	0	0	0.312	0	0	0	0	0	0.312	0	0
O-UB-2	0	0	0	0	0	0.098	0.49	0	0	0	0	0	0	0
O-UB-3	0	0	0	0	0.1	0.07	0.08	0	0	0	0	0	0	0
O-UG-1	0	0	0	0.231	0	0	0	0.603	0	0.083	0	0	0	0
O-UG-1-2	0	0	0	0.071	0	0	0	0	0.49	0.214	0	0.225	0	0
O-UG-2	0	0	0	0.087	0	0	0	0.292	0	0.285	0	0	0	0
O-UK-1	0	0	0	0	0	0	0	0.3	0.3	0	0.25	0	0	0
O-UR-1	0	0	0	0	0	0	0	0.126	0	0	0.13	0.126	0.126	0
OK-1	0	0	0	0	0	0	0	0.655	0	0	0.167	0	0.178	0
R	0	0	0	0	0.05	0	0.1	0	0	0	0	0	0	0.5
REST	0	0	0	0	0	0	0	0	0	0	0	0	0	0
RnM	0	0	0	0	0	0	0	0	0	0	0	0	0	0
RvD	0	0	0	0	0	0	0	0	0	0	0	0	0	0
RvM	0	0	0	0	0	0	0	0	0	0	0	0	0	0
RvO	0	0	0	0	0	0	0	0	0	0	0	0	0	0
RwD	0	0	0	0	0	0	0	0	0	0	0	0	0	0
RwM	0	0	0	0	0	0	0	0	0	0	0	0	0	0
RwO	0	0	0	0	0	0	0	0	0	0	0	0	0	0
RzD	0	0	0	0	0	0	0	0	0	0	0	0	0	0
RzM	0	0	0	0	0	0	0	0	0	0	0	0	0	0
RzO	0	0	0	0	0	0	0	0	0	0	0	0	0	0
U-REST	0	0	0	0	0	0	0	0	0	0	0	0	0	0
UA-1	0	0	0	0	0	0	0	0	0	0.092	0	0	0	0
UA-2	0	0	0	0	0.271	0	0	0	0	0	0	0	0	0
UB-1	0	0	0	0	0	0.08	0	0	0	0	0	0	0	0
UB-2	0	0	0	0	0	0	0	0	0	0	0	0	0	0
UB-3	0	0	0	0	0	0	0	0	0	0	0	0	0	0
UG-1	0	0	0	0	0	0	0	0.322	0	0	0	0	0	0
UG-1-2	0	0	0	0	0	0	0	0.2	0	0	0	0	0	0
UG-2	0	0	0	0	0	0	0	0.062	0	0.127	0	0	0	0
UM-1	0.448	0	0	0	0	0	0	0	0	0	0	0	0	0
UR-1	0	0	0	0	0	0	0	0	0	0	0	0.07	0	0
V.1-2	0	0	0	0	0	0	0	0.14	0	0	0	0.36	0	0
VI.2-3	0.071	0	0	0	0	0	0.156	0	0	0	0	0	0	0
VI.4	0	0	0	0	0	0.267	0.065	0	0	0	0	0	0	0
VI.7	0	0	0	0	0	1	0	0	0	0	0	0	0	0
VI.8	0	0	0	0	0	0.425	0	0	0	0	0	0	0	0
VII.1	0	0	0	0	0	0	0	0.189	0	0	0	0	0	0
VII.1-3	0	0	0	0	0	0	0	0	0	0	0	0.183	0	0
VII.3	0	0	0	0	0	0	0	0.321	0	0	0	0	0	0

ECOCODE	REST	RnM	RvD	RvM	RvO	RwD	RwM	RwO	RzD	RzM	U-REST	UA-1	UA-2	UB-1
H-REST	0	0	0	0	0	0	0	0	0	0	0	0	0	0
HA-1	0	0	0	0	0	0	0	0	0	0	0	0.653	0	0
HA-2	0	0	0	0	0	0	0	0	0	0	0	0	0.049	0
HB-1	0	0	0	0	0	0	0	0	0	0	0	0	0	0.097
HB-2	0	0	0	0	0	0	0	0	0	0	0	0	0	0
HB-3	0	0	0	0	0	0	0	0	0	0	0	0	0.138	0.161
HG-1	0	0	0	0	0	0	0	0	0	0	0	0	0	0
HG-1-2	0	0	0	0	0	0	0	0	0	0	0	0	0	0
HG-2	0	0	0	0	0	0	0	0	0	0	0	0.024	0	0.009
HM-1	0	0	0	0	0	0	0	0	0	0	0	0	0	0
HR-1	0	0	0	0	0	0	0	0	0	0	0	0.093	0	0
I.1	0	0	0	0	0	0	0	0	0	0	0	0	0	0
II.2	0	0	0	0	0	0	0	0	0	0	0	0	0	0
III.2-3	0	0	0	0	0	0	0	0	0	0	0	0	0	0
IV.8-9	0	0	0	0	0	0	0	0	0	0	0	0	0	0
IX.a	0	0	0	0	0	0	0	0	0	0	0	1	0	0
O-U-REST	0	0	0	0	0	0	0	0	0	0	0.2	0.1	0	0
O-UA-1	0	0	0	0	0	0	0	0	0	0	0	0	0	0
O-UA-2	0	0	0	0	0	0	0	0	0	0	0	0	0	0
O-UB-1	0	0	0	0	0	0	0	0	0	0	0	0	0	0
O-UB-2	0	0	0	0	0	0	0	0	0	0	0	0	0.049	0
O-UB-3	0	0	0	0	0	0	0	0	0	0	0	0	0	0
O-UG-1	0	0	0	0	0	0	0	0	0	0	0	0	0	0
O-UG-1-2	0	0	0	0	0	0	0	0	0	0	0	0	0	0
O-UG-2	0	0	0	0	0	0	0	0	0	0	0	0	0	0
O-UK-1	0	0	0	0	0	0	0	0	0	0	0	0	0	0
O-UR-1	0	0	0	0	0	0	0	0	0	0	0	0	0	0
OK-1	0	0	0	0	0	0	0	0	0	0	0	0	0	0
R	0	0	0	0	0	0	0	0	0	0	0	0	0	0
REST	0	0	0	0	0	0	0	0	0	0	0	0	0.315	0
RnM	0	1	0	0	0	0	0	0	0	0	0	0	0	0
RvD	0	0	1	0	0	0	0	0	0	0	0	0	0	0
RvM	0	0	0	1	0	0	0	0	0	0	0	0	0	0
RvO	0	0	0	0	1	0	0	0	0	0	0	0	0	0
RwD	0	0	0	0	0	1	0	0	0	0	0	0	0	0
RwM	0	0	0	0	0	0	1	0	0	0	0	0	0	0
RwO	0	0	0	0	0	0	0	1	0	0	0	0	0	0
RzD	0	0	0	0	0	0	0	0	1	0	0	0	0	0
RzM	0	0	0	0	0	0	0	0	0	1	0	0	0	0
RzO	0	0	0	0	0	0	0	0	0	0	0	0	0	0
U-REST	0	0	0	0	0	0	0	0	0	0	0	0	0	0
UA-1	0	0	0	0	0	0	0	0	0	0	0	0.616	0	0
UA-2	0	0	0	0	0	0	0	0	0	0	0	0	0	0
UB-1	0	0	0	0	0	0	0	0	0	0	0	0	0	0.675
UB-2	0	0	0	0	0	0	0	0	0	0	0	0	0	0
UB-3	0	0	0	0	0	0	0	0	0	0	0	0	0	0.278
UG-1	0	0	0	0	0	0	0	0	0	0	0	0	0	0
UG-1-2	0	0	0	0	0	0	0	0	0	0	0	0	0	0
UG-2	0	0	0	0	0	0	0	0	0	0	0	0	0	0
UM-1	0	0	0	0	0	0	0	0	0	0	0	0	0	0
UR-1	0	0	0	0	0	0	0	0	0	0	0	0	0	0
V.1-2	0	0	0	0	0	0	0	0	0	0	0	0	0	0.03
VI.2-3	0	0	0	0	0	0	0	0	0	0	0	0	0	0
VI.4	0	0	0	0	0	0	0	0	0	0	0	0	0	0.356
VI.7	0	0	0	0	0	0	0	0	0	0	0	0	0	0
VI.8	0	0	0	0	0	0	0	0	0	0	0	0	0	0
VII.1	0	0	0	0	0	0	0	0	0	0	0	0	0	0
VII.1-3	0	0	0	0	0	0	0	0	0	0	0	0	0	0
VII.3	0	0	0	0	0	0	0	0	0	0	0	0	0	0

ECOCODE	UB-3	UG-1	UG-1-2	UG-2	UM-1	UR-1	V.1-2	VI.2-3	VI.4	VI.7	VI.8	VII.1	VII.1-3	VII.3
H-REST	0	0	0	0	0	0	0	0	0	0	0	0	0	0
HA-1	0	0	0	0.109	0	0	0	0	0	0	0	0	0	0
HA-2	0	0	0	0	0	0	0	0	0	0	0	0	0	0
HB-1	0.055	0	0	0	0	0	0	0	0.055	0	0	0	0	0
HB-2	0	0	0	0	0	0.105	0	0	0.161	0	0	0	0	0
HB-3	0	0	0	0	0	0	0	0	0.161	0	0	0	0	0
HG-1	0	0.101	0	0.172	0	0	0	0	0	0	0	0	0	0
HG-1-2	0	0.118	0	0	0	0	0.129	0	0	0	0	0	0	0
HG-2	0	0.084	0	0.288	0	0.027	0	0	0	0	0	0	0	0
HM-1	0	0	0	0	0	0	1	0	0	0	0	0	0	0
HR-1	0	0.093	0	0	0	0.138	0	0	0	0	0	0	0	0
I.1	0	0	0	0	0	0	0	0	0	0	0	0	0	0
II.2	0	0	0	0	0	0	0	0.142	0	0	0	0	0	0
III.2-3	0	0	0	0	0	0	0	0	0	0	0	0	0	0
IV.8-9	0	0	0	0	0	0	0	0.166	0	0	0	0	0	0
IX.a	0	0	0	0	0	0	0	0	0	0	0	0	0	0
O-U-REST	0	0	0	0	0	0	0	0	0	0	0	0	0	0
O-UA-1	0	0	0	0	0	0	0	0	0	0	0	0	0	0
O-UA-2	0	0	0	0.982	0	0	0	0	0	0	0	0	0	0
O-UB-1	0	0	0	0	0	0	0	0.32	0	0	0	0	0	0
O-UB-2	0	0	0	0.049	0	0.098	0	0	0.049	0	0.049	0	0	0
O-UB-3	0.15	0	0	0	0	0.05	0	0	0	0	0	0	0	0
O-UG-1	0	0.083	0	0	0	0	0	0	0	0	0	0	0	0
O-UG-1-2	0	0	0	0	0	0	0	0	0	0	0	0	0	0
O-UG-2	0	0	0	0	0	0.292	0	0	0	0	0	0	0	0
O-UK-1	0	0	0.05	0	0	0	0	0	0	0	0	0	0	0
O-UR-1	0.126	0	0	0	0	0	0	0.367	0	0	0	0	0	0
OK-1	0	0	0	0	0	0	0	0	0	0	0	0	0	0
R	0	0	0	0	0	0	0	0	0	0	0	0	0	0
REST	0	0	0	0	0	0	0	0	0	0	0	0	0	0
RnM	0	0	0	0	0	0	0	0	0	0	0	0	0	0
RvD	0	0	0	0	0	0	0	0	0	0	0	0	0	0
RvM	0	0	0	0	0	0	0	0	0	0	0	0	0	0
RvO	0	0	0	0	0	0	0	0	0	0	0	0	0	0
RwD	0	0	0	0	0	0	0	0	0	0	0	0	0	0
RwM	0	0	0	0	0	0	0	0	0	0	0	0	0	0
RwO	0	0	0	0	0	0	0	0	0	0	0	0	0	0
RzD	0	0	0	0	0	0	0	0	0	0	0	0	0	0
RzM	0	0	0	0	0	0	0	0	0	0	0	0	0	0
RzO	0	0	0	0	0	0	0	0	0	0	0	0	0	0
U-REST	0	0	0	0	0	0	0	0	0	0	0	0	0	0
UA-1	0	0	0	0.184	0	0	0	0	0	0	0	0	0	0
UA-2	0	0	0	0.243	0	0	0	0	0	0	0	0	0	0
UB-1	0	0	0	0	0	0	0	0.03	0.08	0	0	0	0	0
UB-2	0.105	0	0	0	0	0	0	0.123	0	0	0	0	0	0
UB-3	0.346	0	0	0.139	0	0	0	0	0	0	0	0	0	0
UG-1	0	0.21	0	0.096	0	0.192	0	0	0	0	0	0.096	0	0
UG-1-2	0	0.246	0	0.271	0	0	0	0	0	0	0	0	0	0
UG-2	0	0.322	0	0.325	0	0.085	0	0.042	0	0	0	0.036	0	0
UM-1	0	0	0	0	0	0	0.552	0	0	0	0	0	0	0
UR-1	0	0.035	0	0	0	0.627	0.08	0	0	0.094	0	0	0	0
V.1-2	0	0.08	0	0	0	0.229	0	0.16	0	0	0	0	0	0
VI.2-3	0	0	0	0	0	0.097	0	0.352	0.168	0	0	0	0.071	0
VI.4	0	0	0	0	0	0	0	0.032	0.193	0	0	0	0	0
VI.7	0	0	0	0	0	0	0	0	0	0	0	0	0	0
VI.8	0.212	0	0	0	0	0	0	0	0	0	0	0	0	0
VII.1	0	0.378	0	0	0	0	0	0	0	0	0	0.433	0	0
VII.1-3	0	0	0	0	0	0	0	0	0	0	0	0.496	0.183	0
VII.3	0	0.358	0	0	0	0	0	0	0	0	0	0	0	0



## APPENDIX 2 : ECOTOPES BASELINE 4 ROUGHNESS CODES

Ecotope code	Description	Roughness code baseline 4	Roughness code description
HA-1	Highwater free agriculture	121	Agricultural land
HA-2	Highwater free builtup area	114	Paved / Builtup area
HB-1	Highwater free natural forest	1244	Natural forest
HB-2	Highwater free shrubs	1233	Shrubs
HB-3	Highwater free production forest	1242	Production forest
HG-1	Highwater free natural grassland	1202	Natural meadows
HG-1-2	Highwater free grassland (natural or production)	1202	Production / natural meadows
HG-2	Highwater free production grassland	1201	Production meadows
HM-1	Highwater free reeds	1807	Reeds and other helophytes
HR-1	Highwater free herbaceous vegetation	1212	Herbaceous vegetation
H-REST	Highwater free temporarily bare	1250	Rest
I.1	Dynamic sweet to brackish shallow water	106	Shallow water
I.3	Slightly dynamic sweet to brackish shallow water	106	Shallow water
II.1	Gravel bars	111	Bare river bar
II.2	Sweet sand bars	111	Bare river bar
II.2-3	Sweet sand bars/ sweet mud banks	111	Bare river bar
II.3	Sweet mud banks	111	Bare river bar
II.4-5	Mid to highly dynamic brackish and salty bars	111	Bare river bar
III.2	Highly dynamic hard substrate influenced by sweet to brackish water	113	Paved / Builtup area
III.2-3	Low dynamic hard substrate influenced by sweet to brackish water	113	Paved / Builtup area
III.4	Low dynamic hard substrate influenced by brackish water	113	Paved / Builtup area
III.8	Low dynamic hard substrate on the outside berm influenced by salty water	113	Paved / Builtup area
IV.1	Species poor helophytes in shallow sweet water	1807	Reeds and other helophytes
IV.3-IV.8	Species poor helophytes swamp	1224	Bulrush / other helophytes
IV.7	Brackish helophyte culture	1807	Reeds and other helophytes
IV.8-9	Species poor helophytes swamp/Species rich reed swamp	1807	Reeds and other helophytes
IX.a	Agriculture on the shoreline	121	Agricultural land
OK-1	Unvegetated natural levee	1250	Bare levee
O-UA-1	Natural levee or floodplain agriculture	121	Agricultural land
O-UA-2	Natural levee or floodplain builtup area	114	Paved / Builtup area
O-UB-1	Natural levee or floodplain forest	1245	Natural forest
O-UB-2	Natural levee or floodplain shrubs	1231	Shrubs
O-UB-3	Natural levee or floodplain production forest	1242	Production forest
O-UG-1	Natural levee or floodplain grass land	1202	Natural grassland
O-UG-1-2	Natural levee or floodplain grass land (natural or production)	1202	Production / natural meadows
O-UG-2	Natural levee or floodplain production grassland	1201	Production meadows
O-UK-1	Natural levee or floodplain unvegetated	1250	Bare levee
O-UR-1	Natural levee or floodplain herbaceous vegetation	1212	Herbaceous vegetation
O-U-REST	Natural levee or floodplain temporarily bare	1250	Rest
R	Temporarily bare	1250	Rest
REST	Temporarily bare	1250	Rest
REST-O	Temporarily bare	1250	Rest
REST-O-T	Temporarily bare	1250	Rest
REST-T	Temporarily bare high water free	1250	Rest
RnM	Moderately deep side channel	105	Side channel
RnMz-h	Moderately deep side channel	105	Side channel
RnOz-h	Moderately deep side channel	105	Side channel
RvD	(Very) deep	106	River accompanying water
RvDz-k-h	(Very) deep	106	River accompanying water
RvDz-k-h/RvMz-k-h	(Very) deep / moderately deep	106	River accompanying water
RvM	Moderately deep water	106	River accompanying water
RvMz-k-h	Moderately deep water	106	River accompanying water
RvO	Shallow water	106	River accompanying water
RvOz-k-h	Shallow water	106	River accompanying water
RwD	(Very) deep water	106	River accompanying water
RwM	Moderately deep water	106	River accompanying water
RwMz-h	Moderately deep water	106	River accompanying water
RwO	Shallow water	106	River accompanying water

Ecotope code	Description	Roughness code baseline 4	Roughness code description
RwOz-h	Shallow water	106	River accompanying water
RzD	Deep main channel	102	Main channel
RzDz-h	Deep main channel	102	Main channel
RzM	Moderately deep main channel	102	Main channel
RzMz-h	Moderately deep main channel	102	Main channel
RzO	Shallow main channel	102	Main channel
RzOz-h	Shallow main channel	102	Main channel
UA-1	Floodplain agriculture	121	Agricultural land
UA-2	Floodplain builtup area	114	Paved / Builtup area
UB-1	Floodplain forest	1245	Natural forest
UB-2	Floodplain shrubs	1231	Shrubs
UB-3	Floodplain production forest	1242	Production forest
UG-1	Floodplain grass land	1202	Natural grassland
UG-1-2	Floodplain grass land (natural or production)	1202	Production / natural meadows
UG-2	Floodplain production grass land	1201	Production meadows
UG-HA-2	Floodplain production grass land / Highwater free production grass land	114	Production meadow / builtup
U-HG-2	Floodplain production grass land / Highwater free builtup area	1201	Production meadow
UM-1	Natural levee or floodplain reed	1807	Reeds and other helophytes
UR-1	Floodplain herbaceous vegetation	1212	Herbaceous vegetation
U-REST	Floodplain temporarily bare	1250	Rest
V.1-2	Floodplain swamp	1804	Herbaceous vegetation
V.2	Species poor reed swamp	1804	Reeds and other helophytes
V.2/UR-1-2	Species poor reed swamp/floodplain natural grass land/floodplain production grass land	1202	Herbaceous vegetation
V.4/UR-1	Species poor, stucture rich floodplain herbaceous vegetation	1212	Herbaceous vegetation
VI.2	Softwood shrubs	1231	Shrubs
VI.2-3	Softwood shrubs or pioneer softwood forest	1231	Shrubs
VI.4	Softwood forest	1245	Natural forest
VI.5	Floodplain forest	1242	Natural forest
VI.7	Floodplain willow production forest	1232	Willow production forest
VI.8	Production forest on shoreline	1242	Production forest
VI.g	Production / natural grass land	1202	Production / natural meadows
VI.nb	Natural forest	1245	Natural forest
VI.pb	Production forest	1242	Production forest
VII.1	Swampy inundation grass land	1202	Natural grassland
VII.1-2	Swampy inundation grass land / structure rich grass land	1202	Natural grassland
VII.1-2-3	Swampy inundation grass land / structure rich grass land/ production grass land	1202	Production / natural meadows
VII.1-3	Swampy inundation grass land / structure rich grass land/ production grass land	1202	Production / natural meadows
VII.2	Structure rich grass land	1202	Natural meadows
VII.3	Production grass land	1201	Production meadow



## APPENDIX 3 : OVERVIEW OF FIGURES

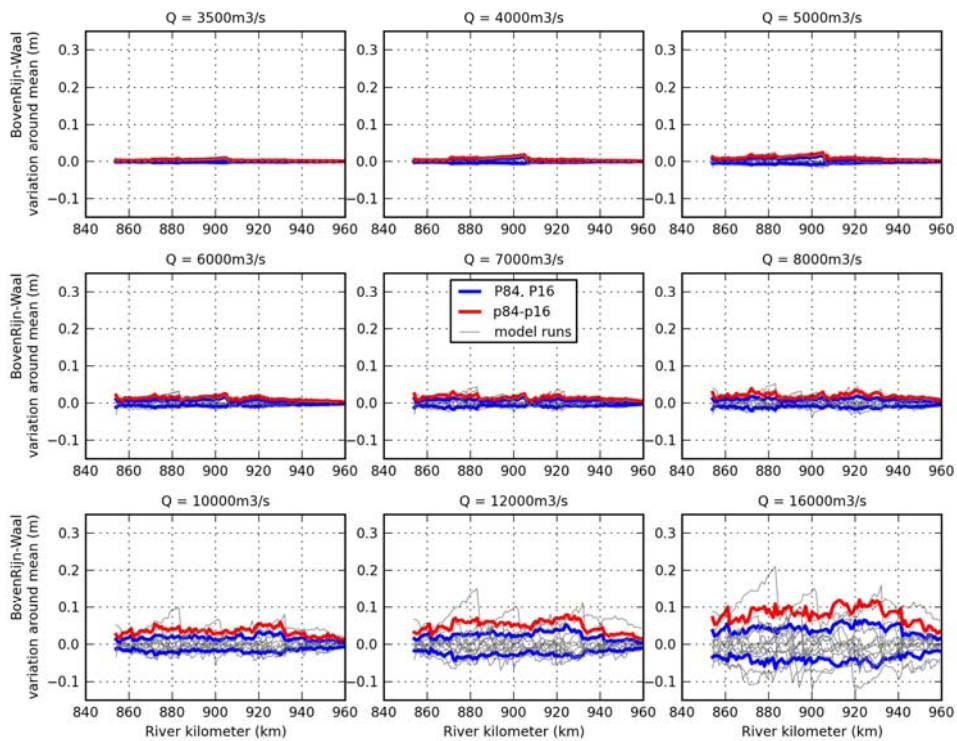


Figure C1 Variability in water levels in the river Waal due to classification error at 69% accuracy.

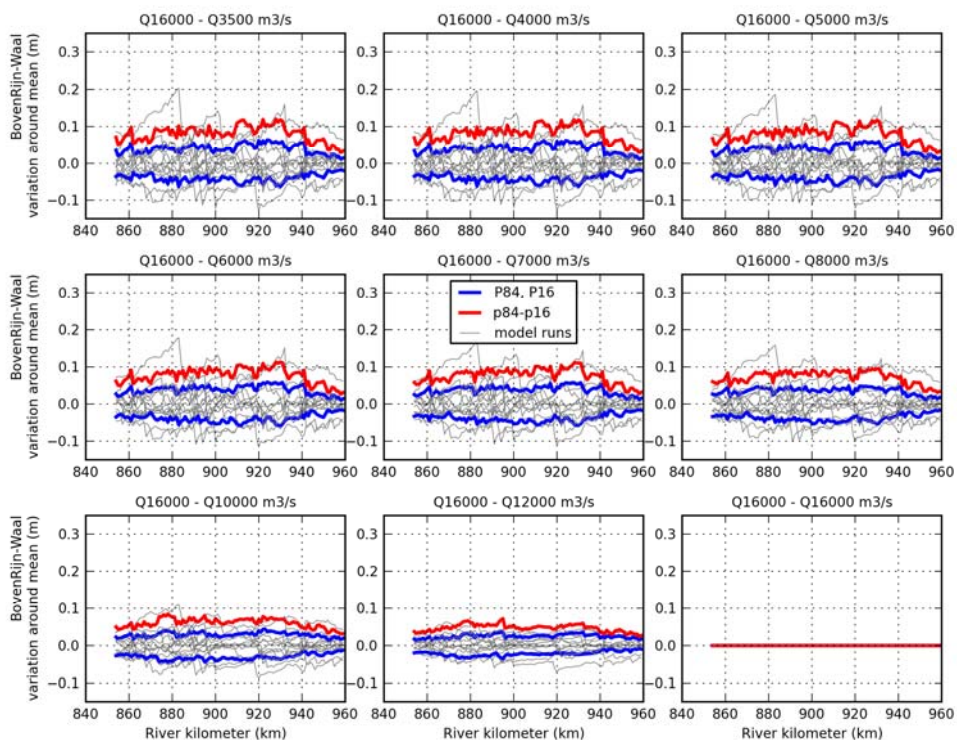


Figure C2 Extrapolation error in water levels in the river Waal due to classification error at 69% accuracy after calibration at different discharges.

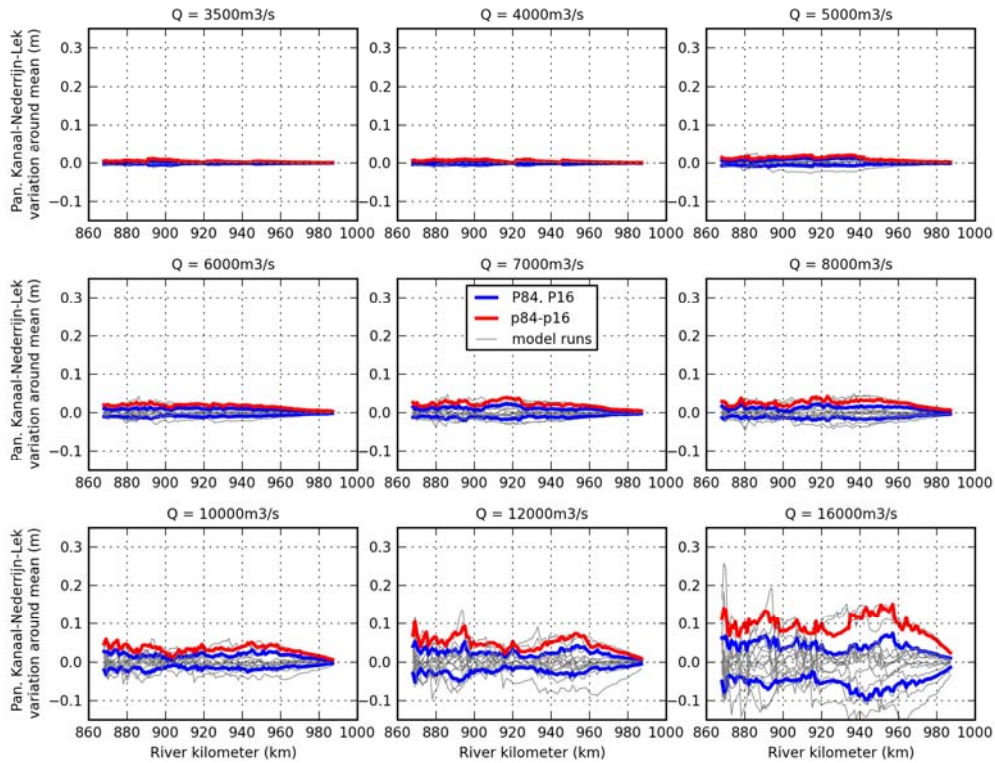


Figure C3 Variability in water levels in the Pannerdensch Kanaal-Nederrijn-Lek due to classification error at 69% accuracy.

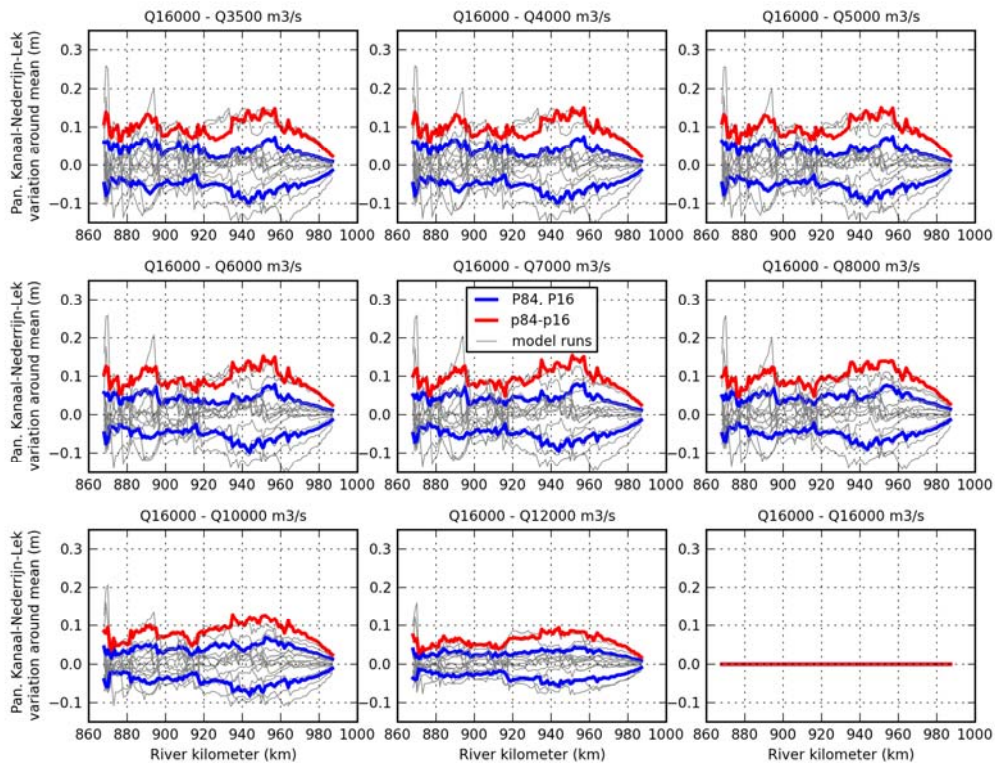


Figure C4 Extrapolation error in water levels in the Pannerdensch Kanaal- Nederrijn-Lek due to classification error at 69% accuracy after calibration at different discharges.

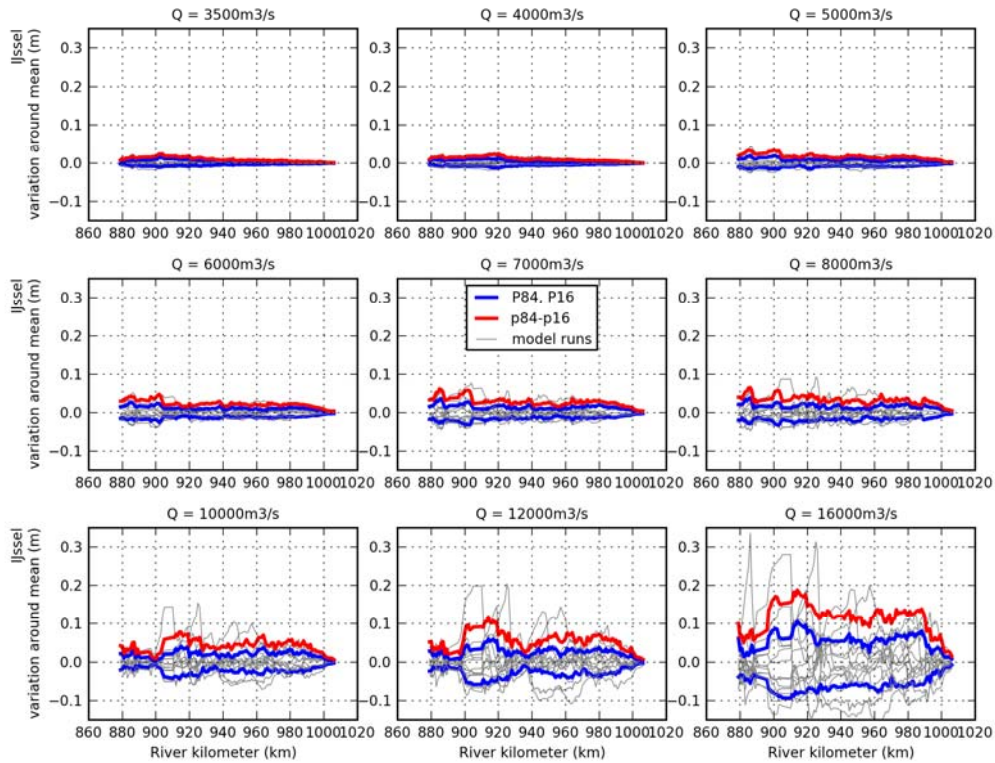


Figure C5 Variability in water levels in the river IJssel due to classification error at 69% accuracy.

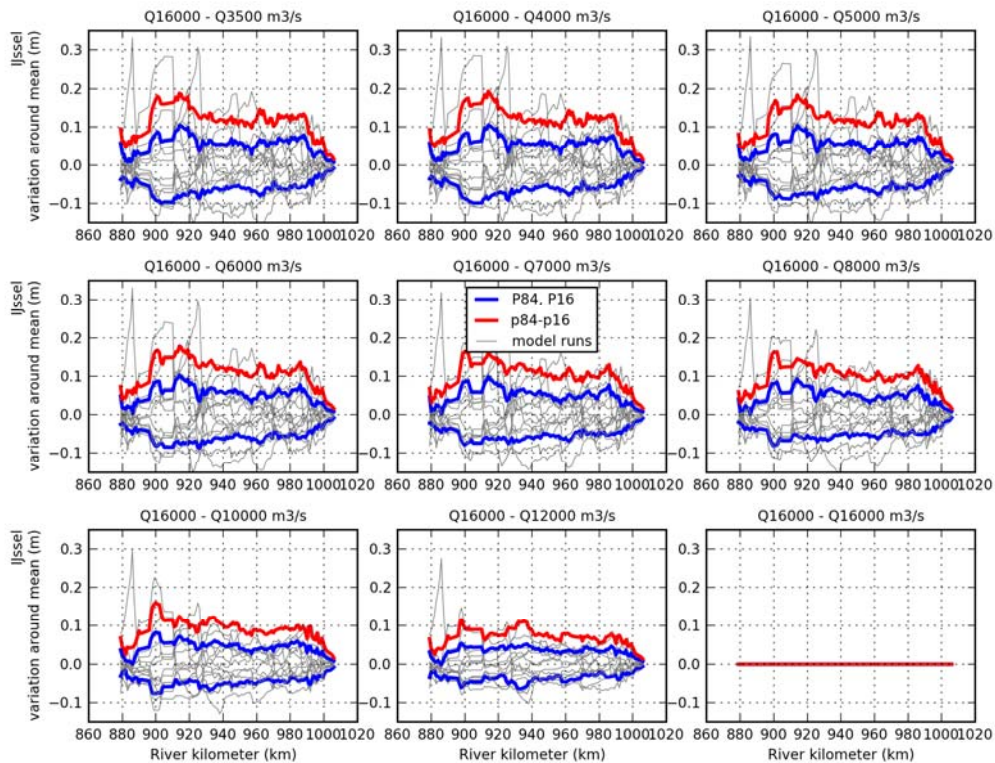


Figure C6 Extrapolation error in water levels in the river IJssel due to classification error at 69% accuracy after calibration at different discharges.



## APPENDIX 4 : EXTRAPOLATION ERROR IN WATER LEVELS

<b>Bovenrijn-Waal</b>		Spread (m)								
<b>69% CA</b>	<b>Q / Q</b>	<b>3500</b>	<b>4000</b>	<b>5000</b>	<b>6000</b>	<b>7000</b>	<b>8000</b>	<b>10000</b>	<b>12000</b>	<b>16000</b>
Range (m)	<b>3500</b>		0.01	0.02	0.02	0.03	0.03	0.06	0.08	0.12
	<b>4000</b>	0.01		0.01	0.02	0.02	0.03	0.06	0.08	0.12
	<b>5000</b>	0.03	0.02		0.01	0.02	0.03	0.05	0.08	0.12
	<b>6000</b>	0.04	0.04	0.03		0.01	0.02	0.05	0.07	0.11
	<b>7000</b>	0.06	0.05	0.05	0.02		0.02	0.05	0.06	0.11
	<b>8000</b>	0.07	0.07	0.06	0.04	0.03		0.03	0.05	0.1
	<b>10000</b>	0.13	0.12	0.11	0.1	0.09	0.07		0.03	0.08
	<b>12000</b>	0.2	0.19	0.18	0.16	0.15	0.14	0.07		0.07
	<b>16000</b>	0.29	0.29	0.28	0.26	0.25	0.23	0.17	0.12	

<b>Pann. Kan.-Nederrijn-Lek</b>		Spread (m)								
<b>69% CA</b>	<b>Q / Q</b>	<b>3500</b>	<b>4000</b>	<b>5000</b>	<b>6000</b>	<b>7000</b>	<b>8000</b>	<b>10000</b>	<b>12000</b>	<b>16000</b>
Range (m)	<b>3500</b>		0.01	0.02	0.03	0.04	0.04	0.06	0.1	0.15
	<b>4000</b>	0.01		0.02	0.02	0.04	0.04	0.06	0.1	0.15
	<b>5000</b>	0.04	0.03		0.02	0.03	0.03	0.05	0.1	0.15
	<b>6000</b>	0.05	0.05	0.03		0.02	0.03	0.05	0.09	0.15
	<b>7000</b>	0.07	0.06	0.05	0.04		0.02	0.05	0.08	0.15
	<b>8000</b>	0.09	0.08	0.07	0.06	0.03		0.05	0.07	0.14
	<b>10000</b>	0.11	0.11	0.1	0.1	0.1	0.09		0.05	0.13
	<b>12000</b>	0.2	0.2	0.2	0.21	0.21	0.2	0.11		0.09
	<b>16000</b>	0.37	0.37	0.36	0.36	0.35	0.35	0.28	0.23	

<b>IJssel</b>		Spread (m)								
<b>69% CA</b>	<b>Q / Q</b>	<b>3500</b>	<b>4000</b>	<b>5000</b>	<b>6000</b>	<b>7000</b>	<b>8000</b>	<b>10000</b>	<b>12000</b>	<b>16000</b>
Range (m)	<b>3500</b>		0.01	0.02	0.04	0.05	0.05	0.08	0.12	0.19
	<b>4000</b>	0.02		0.02	0.04	0.05	0.06	0.09	0.12	0.19
	<b>5000</b>	0.06	0.05		0.02	0.03	0.04	0.07	0.11	0.18
	<b>6000</b>	0.09	0.08	0.04		0.02	0.03	0.07	0.11	0.18
	<b>7000</b>	0.13	0.13	0.08	0.06		0.02	0.05	0.1	0.16
	<b>8000</b>	0.14	0.13	0.11	0.11	0.05		0.04	0.09	0.16
	<b>10000</b>	0.2	0.2	0.19	0.18	0.13	0.09		0.08	0.16
	<b>12000</b>	0.27	0.27	0.25	0.25	0.2	0.17	0.19		0.12
	<b>16000</b>	0.44	0.44	0.43	0.42	0.39	0.37	0.35	0.32	

**Bovenrijn-Waal**

		Spread (m)								
95% CA	Q / Q (m <sup>3</sup> /s)	3500	4000	5000	6000	7000	8000	10000	12000	16000
Range (m)	3500		0	0.01	0.01	0.01	0.01	0.02	0.03	0.05
	4000	0		0	0.01	0.01	0.01	0.02	0.03	0.05
	5000	0.01	0.01		0	0.01	0.01	0.01	0.03	0.04
	6000	0.02	0.02	0.01		0	0.01	0.01	0.02	0.04
	7000	0.02	0.02	0.01	0.01		0.01	0.01	0.02	0.04
	8000	0.03	0.03	0.02	0.02	0.01		0.01	0.02	0.03
	10000	0.04	0.04	0.04	0.03	0.03	0.03		0.01	0.03
	12000	0.06	0.06	0.06	0.06	0.06	0.05	0.03		0.02
	16000	0.1	0.1	0.09	0.09	0.09	0.09	0.07	0.04	

**Pann. Kan.-Nederrijn-Lek**

		Spread (m)								
95% CA	Q / Q (m <sup>3</sup> /s)	3500	4000	5000	6000	7000	8000	10000	12000	16000
Range (m)	3500		0	0.01	0.01	0.01	0.02	0.03	0.04	0.07
	4000	0.01		0.01	0.01	0.01	0.02	0.03	0.03	0.07
	5000	0.01	0.01		0	0.01	0.02	0.02	0.03	0.07
	6000	0.02	0.02	0.01		0.01	0.01	0.02	0.03	0.07
	7000	0.03	0.03	0.02	0.02		0.01	0.02	0.03	0.06
	8000	0.05	0.05	0.04	0.03	0.02		0.02	0.03	0.06
	10000	0.07	0.07	0.07	0.06	0.05	0.04		0.02	0.06
	12000	0.09	0.09	0.09	0.09	0.08	0.07	0.04		0.04
	16000	0.16	0.16	0.16	0.15	0.15	0.14	0.13	0.1	

**IJssel**

		Spread (m)								
95% CA	Q / Q (m <sup>3</sup> /s)	3500	4000	5000	6000	7000	8000	10000	12000	16000
Range (m)	3500		0.01	0.01	0.02	0.02	0.03	0.03	0.04	0.07
	4000	0.02		0.01	0.02	0.02	0.03	0.03	0.04	0.08
	5000	0.02	0.02		0.01	0.01	0.02	0.03	0.04	0.07
	6000	0.03	0.03	0.02		0.01	0.01	0.03	0.04	0.07
	7000	0.04	0.03	0.02	0.02		0.01	0.02	0.03	0.06
	8000	0.04	0.04	0.03	0.03	0.01		0.02	0.03	0.06
	10000	0.08	0.07	0.07	0.06	0.06	0.05		0.01	0.05
	12000	0.11	0.11	0.11	0.1	0.09	0.08	0.04		0.04
	16000	0.22	0.22	0.21	0.21	0.2	0.19	0.15	0.11	



## APPENDIX 5 : EXTRAPOLATION ERROR IN DISCHARGE

**Waal**

		Spread (m <sup>3</sup> /s)								
		Q \ Q								
		3500	4000	5000	6000	7000	8000	10000	12000	16000
69% CA	Range (m <sup>3</sup> /s)	3500	4000	5000	6000	7000	8000	10000	12000	16000
	3500		1	4	8	15	25	32	40	89
	4000	3		3	8	14	24	31	38	88
	5000	6	5		4	11	23	29	36	86
	6000	12	10	7		7	18	25	31	83
	7000	20	20	16	12		11	18	27	86
	8000	30	29	28	26	15		7	26	93
	10000	78	77	74	70	60	55		19	87
	12000	155	155	151	146	138	127	78		76
	16000	338	337	334	330	319	309	263	191	

**Pann. Kan**

		Spread (m <sup>3</sup> /s)								
		Q \ Q								
		3500	4000	5000	6000	7000	8000	10000	12000	16000
69% CA	Range (m <sup>3</sup> /s)	3500	4000	5000	6000	7000	8000	10000	12000	16000
	3500		1	4	9	15	25	31	41	85
	4000	3		3	7	14	24	31	41	84
	5000	6	5		4	11	22	29	39	83
	6000	11	10	6		7	18	26	35	80
	7000	20	19	16	11		11	18	30	84
	8000	30	29	28	26	16		7	27	91
	10000	78	78	74	70	60	55		22	87
	12000	154	152	149	144	135	125	76		69
	16000	336	334	332	327	317	307	261	194	

**Ne-Lek**

		Spread (m <sup>3</sup> /s)								
		Q \ Q								
		3500	4000	5000	6000	7000	8000	10000	12000	16000
69% CA	Range (m <sup>3</sup> /s)	3500	4000	5000	6000	7000	8000	10000	12000	16000
	3500		1	4	6	9	17	28	38	96
	4000	2		3	6	9	17	28	38	96
	5000	5	5		4	7	14	27	37	96
	6000	13	12	8		5	12	26	35	95
	7000	23	22	19	11		8	21	35	97
	8000	41	40	36	28	18		14	32	99
	10000	62	61	59	52	45	36		21	94
	12000	107	106	104	97	89	78	48		65
	16000	219	219	217	209	201	191	164	122	

**IJssel**

		Spread (m <sup>3</sup> /s)								
		Q \ Q								
		3500	4000	5000	6000	7000	8000	10000	12000	16000
69% CA	Range (m <sup>3</sup> /s)	3500	4000	5000	6000	7000	8000	10000	12000	16000
	3500		1	4	7	10	15	23	35	66
	4000	2		4	7	10	15	23	35	64
	5000	5	5		4	8	12	23	35	65
	6000	11	11	7		4	8	23	32	67
	7000	14	15	10	6		4	21	31	69
	8000	23	24	19	14	9		15	28	68
	10000	44	44	38	38	33	28		14	69
	12000	81	80	76	75	70	65	37		55
	16000	156	155	151	150	145	140	112	88	

**Waal**  
95%  
CA  
Range  
(m<sup>3</sup>/s)

Spread (m<sup>3</sup>/s)

Q \ Q (m <sup>3</sup> /s)	3500	4000	5000	6000	7000	8000	10000	12000	16000
3500		1	2	3	3	5	10	25	58
4000	2		1	2	3	5	10	24	57
5000	4	2		1	3	6	10	25	57
6000	6	5	3		3	5	10	24	56
7000	11	11	9	6		3	9	21	53
8000	19	18	16	13	8		9	19	49
10000	25	24	22	20	15	13		11	42
12000	38	38	37	37	35	33	23		30
16000	92	92	91	91	89	87	74	56	

**Pann. Kan**  
95%  
CA  
Range  
(m<sup>3</sup>/s)

Spread (m<sup>3</sup>/s)

Q \ Q (m <sup>3</sup> /s)	3500	4000	5000	6000	7000	8000	10000	12000	16000
3500		1	1	2	3	5	10	24	49
4000	2		1	2	3	5	10	23	48
5000	4	2		1	3	5	11	23	47
6000	7	5	3		2	5	10	22	45
7000	12	10	8	5		3	9	21	43
8000	19	18	16	12	7		9	20	42
10000	26	24	23	20	15	11		11	40
12000	38	38	36	34	31	27	19		24
16000	78	78	77	76	74	71	61	48	

**Ne-Lek**  
95%  
CA  
Range  
(m<sup>3</sup>/s)

Spread (m<sup>3</sup>/s)

Q \ Q (m <sup>3</sup> /s)	3500	4000	5000	6000	7000	8000	10000	12000	16000
3500		1	1	2	4	5	14	24	50
4000	2		1	2	4	5	14	25	50
5000	3	2		2	3	6	14	24	49
6000	4	4	3		2	5	14	24	49
7000	6	7	7	5		3	13	23	49
8000	13	14	14	13	8		12	23	48
10000	33	34	35	34	28	22		11	40
12000	59	60	61	59	54	46	28		29
16000	111	112	113	112	107	100	83	58	

**IJssel**  
95%  
CA  
Range  
(m<sup>3</sup>/s)

Spread (m<sup>3</sup>/s)

Q \ Q (m <sup>3</sup> /s)	3500	4000	5000	6000	7000	8000	10000	12000	16000
3500		1	1	2	4	6	12	18	37
4000	1		1	1	3	6	12	17	37
5000	3	2		1	3	6	11	17	37
6000	4	4	2		2	4	10	16	36
7000	9	8	6	5		3	9	15	35
8000	13	12	10	9	5		6	13	33
10000	29	28	28	27	23	18		9	28
12000	43	42	42	42	37	33	14		21
16000	83	84	83	84	80	76	58	44	

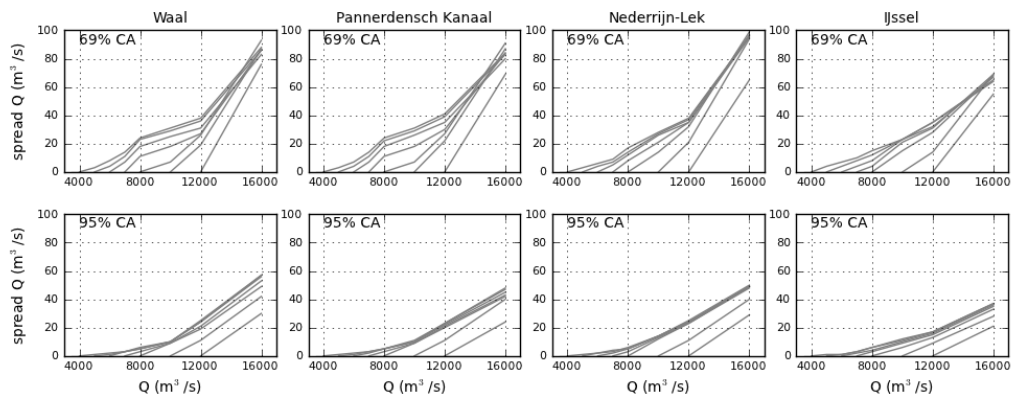


**Figure E1** Spread of the Extrapolation error in discharges between different discharges at 69% classification error (top row) and at 95% classification accuracy (bottom row). Increasing the classification accuracy from 69% to 95% reduces the extrapolation error by 60%. Figure should be read as by following the lines top to bottom: the extrapolation error in the Pannerdensch Kanaal, Nederrijn and Lek is  $87 \text{ m}^3/\text{s}$  when extrapolated from  $10000$  to  $16000 \text{ m}^3/\text{s}$  at 69% CA, and  $41 \text{ m}^3/\text{s}$  when extrapolated from  $10000$  to  $16000 \text{ m}^3/\text{s}$  at 95% CA.

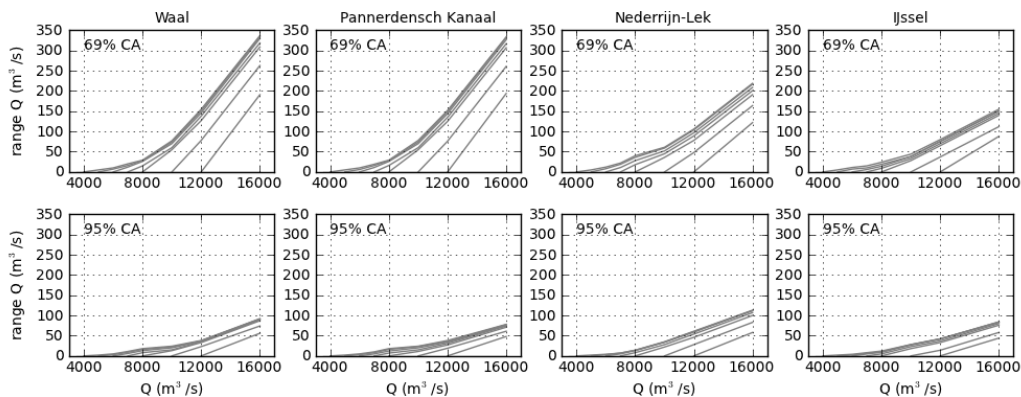


**Figure E2** Range of the Extrapolation error in discharges between different discharges at 69% classification error (top row) and at 95% classification accuracy (bottom row). Figure should be read as by following the lines top to bottom: the range in the extrapolation error in the Pannerdensch Kanaal is  $261 \text{ m}^3/\text{s}$  when extrapolated from  $10000$  to  $16000 \text{ m}^3/\text{s}$  at 69% CA, and  $61 \text{ m}^3/\text{s}$  when extrapolated from  $10000$  to  $16000 \text{ m}^3/\text{s}$  at 95% CA.



## APPENDIX 6 : UNCERTAINTY BOUNDS OF EXTRAPOLATED WATER LEVELS

In this appendix, a practical procedure is described that was used in this study for estimating the error in model predictions of extrapolated flood stages (procedure P2). First, procedure P1 is described, which is the proper but difficult way to calculate uncertainty bounds of extrapolated flood levels. Second, procedure P2 is the more practical way to estimate the uncertainty bounds and involves some simplifying assumptions.

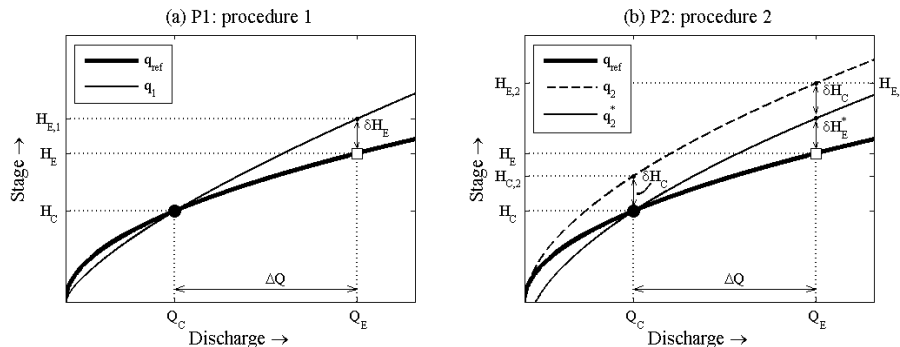


**Figure 17: Extrapolating stage-discharge relations using Procedure 1 and Procedure 2 ( $Q_C$  = calibration discharge level,  $Q_E$  = extrapolation discharge level).**

### 6.1 PROCEDURE P1 (WITH CALIBRATION)

Computational river flow models are typically constructed by assigning (empirically or process-based) roughness descriptors to floodplain land cover and to subsequently calibrate main channel roughness such that the model accurately reproduces recorded stage-discharge levels. Figure 17 shows hypothetical stage-discharge relationships as they may be reproduced by computational flow models. In Figure 17a two stage-discharge relationships are shown, which are both calibrated at discharge  $Q_C$ , yielding the corresponding recorded stage level  $H_C$ . We assume that the relationship depicted by the thick black line is the reference stage-discharge relationship at a particular location along the river  $q_{ref}$ , i.e. the relationship that follows from the calibrated flow model using the standard floodplain land cover map. The other curve,  $q_1$ , is the stage-discharge relationship that corresponds to an alternative set of floodplain and main channel roughnesses, but which also goes through the calibration point at  $(Q_C, H_C)$ .

Following Julien (2002), a river's stage-discharge relationship can typically be approximated by a power-type law. For example, for the reference stage-discharge relation in Figure 17a this would give:

$$q_{ref} = \alpha_C H_C^\beta \quad 1$$

Julien (2002, p.56) states that in this power law that  $\alpha_C$  may be interpreted as the (calibrated) effective resistance coefficient and that exponent  $\beta$  is representative of overland flow characteristics (i.e. floodplain roughness). The reason for attributing floodplain characteristics mainly to  $\beta$  is that  $\beta$  has most influence on the shape of the power law at high  $Q$  values. On the other hand,  $\alpha_C$  influences the shape of the curve over the entire  $Q$ -range. Following this interpretation, we assume that a change in floodplain roughness affects exponent  $\beta$ , and that  $\alpha_C$  is adjusted such that proper calibration at out-of-bank flows is maintained. For example, the thin black line in Figure 17a shows an alternative stage-discharge relationship  $q_1$ , based on a different floodplain roughness map, which has also been recalibrated by adjustment of  $\alpha_C$  to reproduce the recorded flood event  $(Q_C, H_C)$ . For the alternative stage-discharge relationship the floodplain roughness is slightly different from  $q_{ref}$ . This difference is reflected in a difference  $\Delta\beta$  in the exponent of the power law for  $q_1$ :

$$q_1 = \alpha_1 H_C^{\beta + \Delta\beta} \quad 2$$

The value of  $\alpha_1$  follows from the condition that both  $q_1$  and  $q_{ref}$  give water level  $H_C$  if  $q_1 = q_{ref} = Q_C$ :

$$\alpha_1 = \alpha_C H_C^{-\Delta\beta} \quad 3$$

Inserting Equation 3 into Equation 2 gives

$$q_1 = \alpha_C H_C^{-4\beta} h^{\beta+4\beta} \quad 4$$

At discharge levels that lie beyond the calibration discharge  $Q_C$  the two relationships  $q_{ref}$  and  $q_1$  deviate from each other. If we consider the discharge level  $Q_E$  (E stands for 'extrapolation'), the value  $\delta H_E$  represents the difference in water levels between the two stage-discharge relationships at discharge  $Q_E$ :

$$\delta H_E = H_{E,1} - H_E \quad 5$$

The water level  $H_{E,1}$  can be expressed in terms of  $H_E$  by evaluating Equation 1 and Equation 4 at discharge  $Q_E$ :

$$Q_E = \alpha_C H_E^\beta = \alpha_C H_C^{-4\beta} H_{E,1}^{\beta+4\beta} \quad 6$$

from which it follows that

$$H_{E,1} = H_C^{\frac{\beta}{\beta+4\beta}} H_E^{\frac{4\beta}{\beta+4\beta}} \quad 7$$

Inserting Equation 7 into Equation 5 gives

$$\delta H_E = H_C^{\frac{\beta}{\beta+4\beta}} H_E^{\frac{4\beta}{\beta+4\beta}} - H_E = H_E \left( \left( \frac{H_C}{H_E} \right)^{\frac{\beta}{\beta+4\beta}} - 1 \right) \quad 8$$

For each instance of possible floodplain roughness maps the value  $\delta H_E$  can be determined. Next, from the entire set of  $\delta H_E$ -values a probability distribution around the reference extrapolated flood level  $H_E$  follows, together with typical statistical parameters such as the standard deviation and percentile values around  $H_E$ . Using this procedure, uncertainty bounds around  $H_E$  may be determined for each location along the river, giving the 'true extrapolation error' around flood water levels. However, there is a major practical disadvantage of the described approach: if a 2D hydrodynamic river model is used to calculate the  $\delta H_E$ -values, the hydraulic model needs to be recalibrated for each new floodplain roughness map (i.e. for each  $\Delta\beta$ ) such that at all locations along the river the condition ( $Q_C, H_C$ ) is met. This recalibration procedure is difficult and very time consuming. Therefore, in the current study an alternative approach was used to estimate  $\delta H_E$ , which avoids the recalibration step.

## 6.2 PROCEDURE P2 (WITHOUT CALIBRATION)

Procedure P2 is the method used in this study to estimate extrapolation errors around predicted water levels at design discharges. In procedure P2 non-calibrated stage-discharge relationships are used to estimate  $\delta H_E$ -values. Subsequently, in a comparison with procedure P1 it will be assessed how well procedure P2 performs in estimating uncertainty bounds around the extrapolated flood level  $H_E$ . In Figure 17b, a stage-discharge relationship  $q_2$  is shown (dashed line) that corresponds to a new floodplain roughness map, which changes the exponent  $\beta$  by an amount  $\Delta\beta$  but, as opposed to procedure P1, maintains the value of the resistance coefficient  $\alpha_C$ :

$$q_2 = \alpha_C h^{\beta+\Delta\beta} \quad 9$$

Next, instead of recalibrating Equation 9 by adjusting  $\alpha_C$ , an estimate of  $\delta H_E$  (denoted by  $\delta H_E^*$ ) is made by using the rates of change in water levels of  $q_{ref}$  and  $q_2$  between discharge values  $Q_C$  and  $Q_E$ . For this purpose,  $q_2$  is shifted vertically by an amount  $\delta H_C = H_{C,2} - H_C$ , such that at ( $Q_C, H_C$ ) the shifted relationship intersects with  $q_{ref}$ . Effectively,  $\delta H_E^*$  is the change in water level difference when extrapolating from  $Q_C$  to  $Q_E$  between the two model cases with different roughness maps. The shifted stage-discharge relationship is denoted by  $q_2^*$  (the thin solid line in Figure 17b). Next, the quantity  $\delta H_E^*$  is calculated as

$$\delta H_E^* = H_{E,2} - H_E - \delta H_C \quad 10$$

Here  $H_{E,2}$  and  $H_E$  are the water levels at discharge  $Q_E$  for relationships  $q_{ref}$  and  $q_2$  and  $\delta H_C$  is the corresponding difference in water levels at discharge level  $Q_C$  ( $\delta H_C = H_{C,2} - H_C$ , see Figure 17b). Calculating  $\delta H_E^*$  does not require any recalibration and is thus much easier to calculate than  $\delta H_E$  in Equation 5.  $\delta H_E^*$  forms the basis of the percentile values in Chapter 5 of this study.

### Comparing procedures P1 and P2; a correction factor for P2

We compare  $\delta H_E^*$  with  $\delta H_E$  in order to find out how much they differ and to see whether Procedure 2 may be used to estimate as a simplified way to estimate uncertainty bounds around the extrapolated flood water level  $H_E$  (i.e. by using calculated values of  $\delta H_E^*$  to estimate  $\delta H_E$ ). For this purpose, we introduce a proportionality factor  $f$  between  $\delta H_E$  and  $\delta H_E^*$ :

$$\delta H_E = f \delta H_C^* \quad 11$$

As previously done for  $q_1$  in Equations 6 and 7 we evaluate  $q_2$  at discharge levels  $Q_C$  and  $Q_E$  in order to describe  $H_{C,2}$  and  $H_{E,2}$  in terms of  $H_C$  and  $H_E$ :

$$Q_C = \alpha_C H_C^\beta = \alpha_C H_{C,2}^{\beta+\Delta\beta} \rightarrow H_{C,2} = H_C^{\frac{\beta}{\beta+\Delta\beta}} \quad 12$$

$$Q_E = \alpha_C H_E^\beta = \alpha_C H_{E,2}^{\beta+\Delta\beta} \rightarrow H_{E,2} = H_E^{\frac{\beta}{\beta+\Delta\beta}} \quad 13$$

Inserting the derived expressions for  $H_{C,2}$  and  $H_{E,2}$  into Equation 10 yields

$$\delta H_E^* = H_E \left( H_E^{\frac{-\Delta\beta}{\beta+\Delta\beta}} - 1 \right) - H_C \left( H_C^{\frac{-\Delta\beta}{\beta+\Delta\beta}} - 1 \right) \quad 14$$

Next, combining Equations 8, 11 and 14 gives for the proportionality factor

$$f = \frac{\delta H_E}{\delta H_C^*} = \frac{H_E \left( \left( \frac{H_C}{H_E} \right)^{\frac{-\Delta\beta}{\beta+\Delta\beta}} - 1 \right)}{H_E \left( H_E^{\frac{-\Delta\beta}{\beta+\Delta\beta}} - 1 \right) - H_C \left( H_C^{\frac{-\Delta\beta}{\beta+\Delta\beta}} - 1 \right)} \quad 15$$

To evaluate  $f$ , we assume that  $\Delta\beta$  is small compared to  $\beta$ , which allows us to linearize the power law terms in Equation 15 with respect to  $\Delta\beta/\beta$ . By making use of the first order Taylor expansion

$$A^{\frac{\Delta\beta}{\beta+\Delta\beta}} \sim A^{\frac{\Delta\beta}{\beta}} \sim 1 + \frac{\Delta\beta}{\beta} \ln A \quad 16$$

we obtain

$$f \sim \frac{H_E \ln\left(\frac{H_C}{H_E}\right)}{H_C \ln(H_C) - H_E \ln(H_E)} = \frac{\ln\left(\frac{H_C}{H_E}\right)}{\frac{H_C}{H_E} \ln(H_C) - \ln(H_E)} \quad 17$$

Next, we rewrite  $H_C$  and  $H_E$  in terms of  $Q_C$  and  $Q_E$  by using the reference stage-discharge relation given by Equation 1:

$$H_C = \left( \frac{Q_C}{\alpha_C} \right)^{1/\beta} \quad 18$$

$$H_E = \left( \frac{Q_E}{\alpha_C} \right)^{1/\beta} = \left( \frac{Q_C + \Delta Q}{\alpha_C} \right)^{1/\beta} \quad 19$$

In Equation 19 the quantity  $\Delta Q$  is introduced, which is the discharge interval beyond which  $Q_C$  is extrapolated ( $Q_E = Q_C + \Delta Q$ ). Inserting Equations 18 and 19 into 17 gives

$$f \sim \frac{\ln\left(\frac{Q_C}{Q_C + \Delta Q}\right)}{\left(\frac{Q_C}{Q_C + \Delta Q}\right)^{1/\beta} \ln\left(\frac{Q_C}{\alpha_C}\right) - \ln\left(\frac{Q_C + \Delta Q}{\alpha_C}\right)} = \frac{-\ln\left(1 + \frac{\Delta Q}{Q_C}\right)}{\left(1 + \frac{\Delta Q}{Q_C}\right)^{-1/\beta} \ln\left(\frac{Q_C}{\alpha_C}\right) - \ln\left(\frac{Q_C}{\alpha_C} \left(1 + \frac{\Delta Q}{Q_C}\right)\right)} \quad 20$$

The final step is to linearize  $f$  with respect to  $\Delta Q/Q_C$ . This is allowed if  $\Delta Q$  is much smaller than  $Q_C$  or if  $q_{ref}$  and  $q_2$  are nearly linear beyond discharge level  $Q_C$ . The following linearizations are used:

$$\left(1 + \frac{\Delta Q}{Q_C}\right)^{-1/\beta} \sim 1 - \frac{1}{\beta} \frac{\Delta Q}{Q_C} \quad 21$$

and

$$\ln\left(1 + \frac{\Delta Q}{Q_C}\right) \sim \frac{\Delta Q}{Q_C} \quad 22$$

Inserting Equations 21 and 22 into Equation 20 yields

$$f \sim \frac{1}{1 + \frac{1}{\beta} \ln\left(\frac{Q_C}{\alpha_C}\right)} \quad 23$$

Note that  $f$  is now no longer dependent on  $\Delta\beta$  or  $\Delta Q$  and that the proportionality between  $\delta H_E$  and  $\delta H_C^*$  can be estimated by knowing the approximate shape of the reference stage discharge relation  $q_{ref}$ , as characterized by  $\alpha_C$  and exponent  $\beta$ .

### 6.3 QUANTIFICATION OF THE PROPORTIONALITY FACTOR $f$ FOR THE RHINE BRANCHES

The proposed procedure P2 to estimate  $\delta H_E$  by calculating  $f^* \delta H_E^*$  (Equation 11, using Equation 23 for  $f$ ) is applied to the case of the Dutch Rhine branches. In Figure 18 regression curves of type  $Q = \alpha H^\beta$  are shown for four gage stations in the Rhine. It can be seen that the coefficients in the fitted stage-discharge relations differ significantly between the four stations. In each of the four subfigures, the point in the graph with highest discharge value is the flood design discharge ( $Q_E$ ). The data points marked with black circles are the highest recorded discharge values that are available for model calibration ( $Q_C$ ). Figure 19 shows the values for factor  $f$  as based on Equation 23 for the four stations on the Rhine branches. The four lines in the graph correspond to the stage-discharge relations in Figure 18 and depict the  $f$ -values if the  $Q_C$  were either higher or lower at the particular gage station. It appears that  $f$  varies within a relatively confined range of 0.25 to 0.45. Therefore a constant value of  $f=0.3$  seems appropriate to approximately describe the correction factor for the entire Rhine branches.

### 6.4 CONCLUSION

The simplified procedure used in this study to estimate uncertainty bounds of extrapolated flood levels (procedure P2) approximately describes the “true uncertainty bounds” that were found if the proper procedure including recalibration of the model were used (procedure P1). The differences between the outcomes of the procedures can be reduced by adopting a newly introduced correction factor  $f$ . For the Dutch Rhine branches this correction factor would have an approximate value of 0.3, but is different for each location along the river. The consequence of applying procedure P2 but not using a correction factor (i.e. adopting  $f = 1$ , as has been done in this study) results in an overestimation of the uncertainty bounds. The results stated in this study thus give a conservative (maximal) estimate of uncertainty bounds of extrapolated flood water levels.

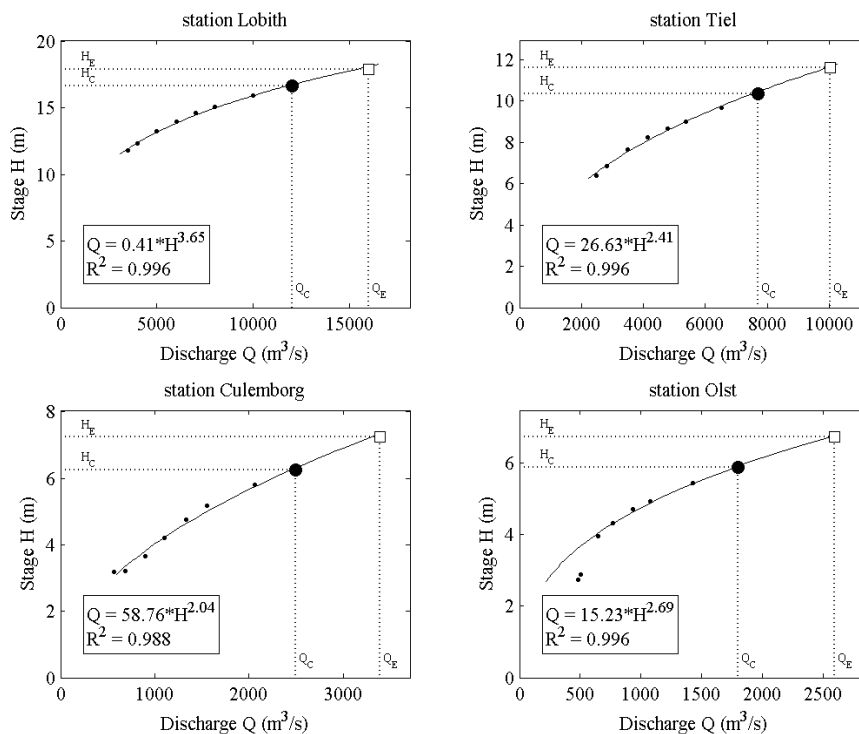


**Figure 18:** Fitted stage-discharge relations at four stations in the Dutch Rhine branches. The plotted points are results from a calibrated 2D hydrodynamic simulation.

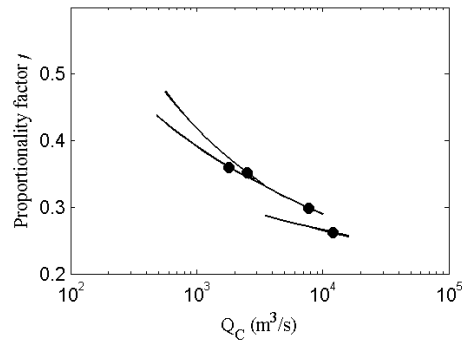


**Figure 19:** Proportionality factor  $f$  for the four stations in the Rhine branches. The black dots correspond to the maximum discharge levels that were used for model calibration.

**Reference**

Julien, P.Y. (2002), River Mechanics, Cambridge University Press, 434p.